EXPERIMENTAL INVESTIGATION ON SHARP CRESTED RECTANGULAR WEIRS

A THESIS SUBMITED TO
THE GRADUATE SCHOOL OF NATURAL AND APPLIED SCIENCES
OF
MIDDLE EAST TECHNICAL UNIVERSITY

BY

SIAMAK GHARAHJEH

IN PARTIAL FULFILENT OF THE REQUIRMENTS
FOR
THE DEGREE OF MASTER OF SCIENCE
IN
CIVIL ENGINEERING

JUNE 2012

Approval of the thesis:

EXPERIMENTAL INVESTIGATION ON SHARP CRESTED RECTANGULAR WEIRS

submitted by **SIAMAK GHARAHJEH** in partial fulfillment of the requirements for the degree of **Master of Science in Civil Engineering Department, Middle East Technical University** by,

Prof. Dr. Canan Özgen _____
Dean, Graduate School of **Natural and Applied Sciences**

Prof. Dr. Güney Özcebe _____
Head of Department, **Civil Engineering**

Prof. Dr. İsmail Aydın _____
Supervisor, **Civil Engineering Dept., METU**

Assoc. Prof. Dr. A.Burcu Altan Sakarya _____
Co-Supervisor, **Civil Engineering Dept., METU**

Examining Committee Members:

Prof. Dr. Nuray Denli Tokyay _____
Civil Engineering Dept., METU

Prof. Dr. İsmail Aydın _____
Civil Engineering Dept., METU

Assoc. Prof. Dr. A.Burcu Altan Sakarya _____
Civil Engineering Dept., METU

Assoc. Prof. Dr. Mehmet Ali Kökpınar _____
Civil Engineering Dept., METU

Dr. Gülizar Özyurt _____

Date: 13 June 2012

I hereby declare that all information in this document has been obtained and presented in accordance with academic rules and ethical conduct. I also declare that, as required by these rules and conduct, I have fully cited and referenced all material and results that are not original to this work.

Name, Last name: Siamak Gharahjeh

Signature:

ABSTRACT

EXPERIMENTAL INVESTIGATION ON SHARP-CRESTED RECTANGULAR WEIRS

Gharahjeh, Siamak
M.Sc., Department of Civil Engineering
Supervisor: Prof. Dr. İsmail Aydin
Co-Supervisor: Assoc. Prof. Dr. A. Burcu Altan-Sakarya

June 2012, 76 pages

This study is an experimental research to formulate the discharge over sharp-crested rectangular weirs. Firstly, a series of measurements on different weir heights were conducted to find the minimum weir height for which channel bed friction has no effect on discharge capacity. After determining the appropriate weir height, weir width was reduced to collect data on discharge-water head over weir relationship for a variety of different weir openings. Then, the data was analyzed through regression analysis along with utilization of global optimization technique to reach the desired formulation for the discharge. By taking advantage of a newly-introduced "weir velocity" concept, a simple function was eventually detected for the discharge where no discharge coefficient was involved. The behavior of the weir velocity function obtained in the present study illustrates the transition between the fully contracted and partially contracted weirs. In addition, the proposed weir velocity formulation is simple and robust to calculate the discharge for full range of weir widths.

Key words: Open channel flow, Flow measurement, Sharp-crested rectangular weir, Contracted weir, Slit weir.

ÖZ

DİKDÖRTGEN KESİTLİ KESKİN KENARLI SAVAKLAR ÜZERİNE DENEYSEL BIR ARAŞTIRMA

Gharahjeh, Siamak

Yüksek Lisans, Inşaat Mühendisliği Bölümü
Tez Yöneticisi : Prof. Dr. İsmail Aydın
Ortak Tez Yöneticisi : Doç. Dr. A. Burcu Altan-Sakarya

Haziran 2012, 76 sayfa

Bu çalışma keskin kenarlı dikdörtgen savaklar üzerinden geçen debiyi bulmak için yapılan deneysel bir araştırmadır. Öncelikle, kanal tabanındaki sürtünmenin debi üzerinde etkisinin olmadığı en küçük savak yüksekliğini bulmak için farklı yükseklikte savaklarla bir seri ölçüm gerçekleştirilmiştir. Uygun savak yüksekliği belirlendikten sonra, savak genişliği daraltılarak savak üstü su derinliği-debi ilişkisini bulmak için farklı savak açıklıklarında veri toplanmıştır. Deneylerden elde edilen veriler regresyon analizinde toplamda optimizasyon yöntemi uygulanarak debi için istenen formul bulunmuştur. Sonuçta, yeni tanımlanan 'savak hızı' kavramından yararlanarak debi katsayısı içermeyen basit bir debi ifadesi bulunmuştur. Bu çalışmadan elde edilen savak hızı fonksiyonunun davranışı, kısmen ve tamamen daraltılımış savaklar arasındaki geçişi göstermektedir. Ayrıca, önerilen savak hızı ifadesi debi hesabı için basit ve kullanışlı olup tüm savak genişlikleri için uygulanabilir.

Anahtar Kelimeler: Açık kanal akımı, Akım ölçümleri, Dikdörtgen kesitli Keskin kenarlı savak, Daralmiş savak, Dar savak.

ACKNOWLEDGMENTS

I would like to sincerely thank my Supervisor Prof. Dr. İsmail Aydın and my Co-Supervisor Assoc. Prof. Dr. A.Burcu Altan-Sakarya for their advice, help and guidance throughout the research. I am very lucky to have known them and gained so many advantages from their pure and deep knowledge.

I am also thankful for my parents' support and patience.

Likewise, I want to express my appreciation towards Prof. Dr. Nuray Denli Tokyay for I have learned so much from her powerful knowledge.

Finally, I am grateful for the assistance of technicians in the laboratory during my experiments and assistants in the department.

To My Family

TABLE OF CONTENTS

LIST OF FIGURES

FIGURES

LIST OF TABLES

TABLES

LIST OF SYMBOLS

b	: Weir opening width
b_e	: Effective weir opening width
B	: Width of the channel
c	: Coefficient term in weir velocity formula
c_c	: Weir velocity correction coefficient in contracted weirs
c_s	: Weir velocity correction coefficient in slit weirs
C_c	: Contraction coefficient
C_d	: Discharge coefficient
C_e	: Effective discharge coefficient
e	: Power term in weir velocity formula
g	: Gravitational acceleration
γ	: Specific weight of the fluid
h_e	: Effective water head on the weir
h'	: Distance of free water surface to the point B
K_b	: Quantity represents the effect of viscosity and surface tension
K_h	: Quantity represents the effect of viscosity and surface tension
ν	: Kinematic viscosity of fluid

L	: Weir width
P	: Weir height
p_A	: Pressure at point A
p_B	: Pressure at point B
q	: Unit discharge per crest length
Q	: Discharge
R	: Reynolds number
R'	: Radius of the circular weir
ρ	: Mass density of the fluid
σ	: Surface tension
u	: Average velocity in the channel
$u_2(h)$	: Velocity at section 2 as a function of h
U_1	: Maximum velocity on the circular weir crest
V_1	: Velocity at section 1
V_{wc}	: Weir velocity for contracted weirs
V_{ws}	: Weir velocity for slit weirs
W_e	: Weber number
w	: Cross-channel width
z_A	: Elevation of the point A
z_B	: Elevation of the point B

CHAPTER 1

INTRODUCTION

1.1. General

The rectangular sharp-crested weirs are of fundamental importance in hydraulic engineering because they serve as the simple, accurate and classical devices used both in the field and laboratory for flow measurements in the open channels.

However, weirs must be calibrated experimentally before useing in the practice. For many years this calibration issue has been the subject of numerous theoretical and experimental investigations by many scientists. In this experimental study which is planned to be complementary to the earlier researches, a wide range of data is collected with the emphasis given to high weir heads in fully contracted slit weirs.

1.2. Scope of the Present Study

In this study, sharp-crested rectangular weirs are experimentally studied. Several series of experiments are carried out in the Hydromechanics Laboratory to investigate various hydraulic characteristics. Initially the location of the weir plate for full width case was determined at the canal exit section. Then, weir height was tested for a couple of different weir sizes to make sure the selected height would be acting as the control section. That is, flow is free from bottom boundary effects for that certain weir height. After fixing the plate height, experiments continued with changing the weir opening, starting from full width to slit weir cases.

In Chapter 2 theoretical considerations of the subject is explained in detail. In Chapter 3 earlier investigations made by other researchers will be discussed and later on they will be used to make comparisons with the present study. Chapter 4 will focus on the procedures and experimental installations of the laboratory study. Chapter 5 is dedicated to the presentation of results and their comparisons with other studies. In the final chapter, conclusions are made by data interpretation and analysis.

CHAPTER 2

THEORETICAL CONSIDERATION

2.1. Definition

The sharp-crested rectangular weir is a vertical plate mounted at right angle to the flow having a sharp-edged crest. While flow passes from over the weir, this section fixes a relationship between flow depth and discharge making it a control section. Because the edge is sharp, it is less likely that a boundary-layer can develop at the upstream vicinity of the weir face and therefore it is possible to assume the flow to be greatly free from viscous effects and subsequent energy losses. Another fundamental interest lays in their theory of which forms the basis of spillways design (Henderson, 1966).

Sharp-crested rectangular weirs can be fallen into three major groups depending on the weir opening (Bos, 1989):

1- Fully contracted weirs: Their operation is not affected by the side walls or bed and the weir opening (b) is less than the channel width (B).

2- Partially contracted weirs: Are slightly effected by the side walls.

3- Full width weirs: Have an opening of equal to channel width (b=B) and can be referred to as suppressed weirs, if sidewalls of the channel extend to downstream of the weir section.

Weirs are identified by their opening shapes. They also can be either broad or sharp crested. For sharp crested weirs, typical shapes include rectangular, triangular and trapezoidal weirs, as indicated in the Figure 2.1.

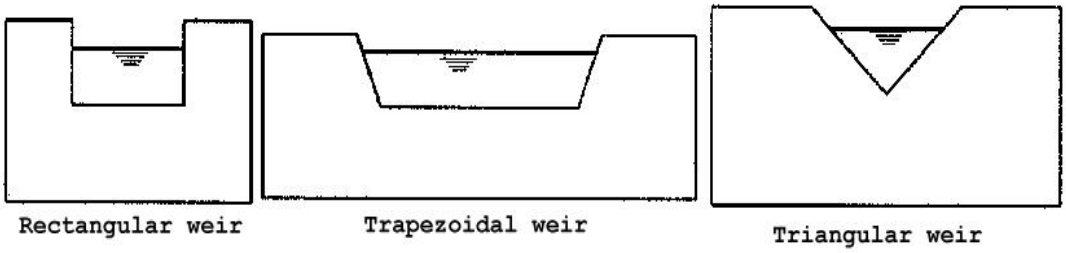

Figure 2.1 Typical shapes of sharp crested weirs

Generally, weir plate should be thin and beveled at some 60° to get the flow separated down the edge forming the lower nappe (Figure 2.2).

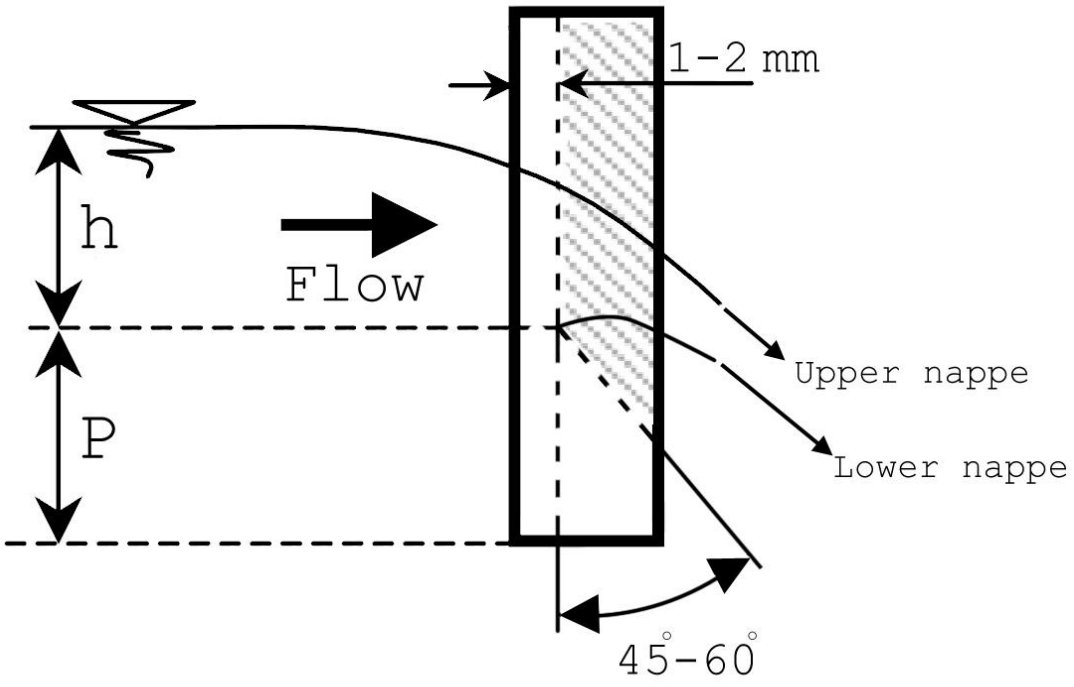

Figure 2.2 Cross-sectional details of sharp crested weir

Air supply at the vicinity of the nappe is essential for the precise measurement of flow, this is termed as aerated nappe (Franzini and Finnemore, 1997). If nappe is non-aerated, water will cling to the weir plate making it impossible to function properly. Therefore in experiments water head was adjusted deep enough to avoid non-aerated nappes.

Figure 2.3 shows the experimental set up of the weir in the laboratory. On the figure, parameters defining the weir and the channel characteristics are illustrated. P is the weir plate height, B is the main channel width, b is the opening of the weir and h is the water head which is measured at a

distance of four times the maximum water head upstream the weir as suggested by Bos (1989).

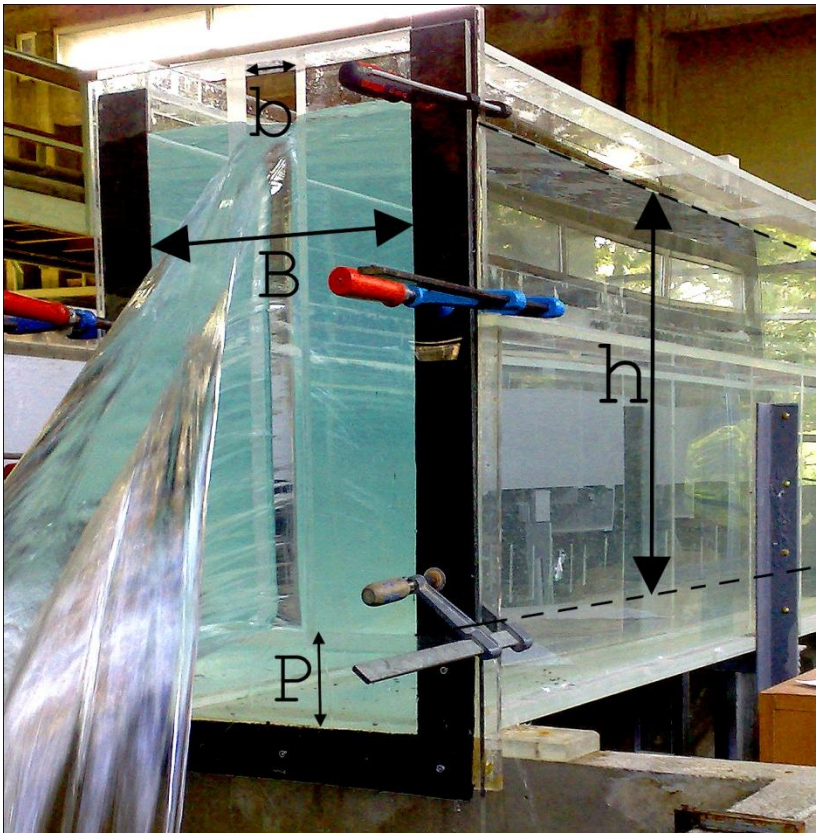

Figure 2.3 Parameters of the sharp-crested rectangular weir

2.2. Discharge Equation Derivation

The complex nature of the flow over the weir is the primary reason of failure in obtaining an exact analytical expression in terms of weir parameters to describe the weirs' functionality. The main mechanisms controlling the flow over the weir are gravity and inertia. Viscous and surface tension effects are of secondary importance, but experimentally determined coefficients are often used to account for these effects (Munson et al., 2002).

As an initial approximation, we assume the velocity profile upstream of the weir to be uniform and the pressure within the nappe is atmospheric as indicated in Figure 2.4.

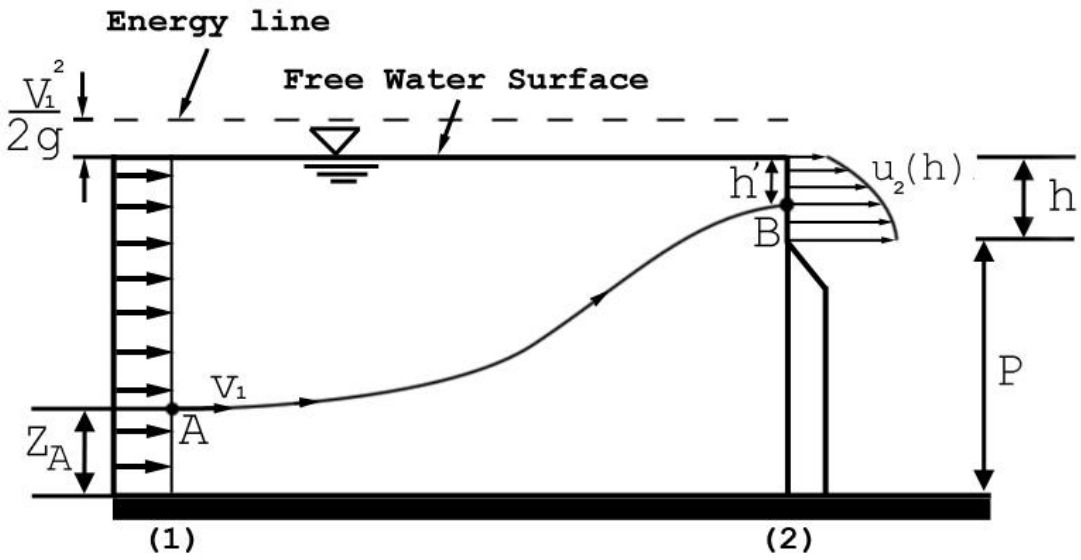

Figure 2.4 Schematic side view of flow over the weir

In addition, we may assume that the fluid flows horizontally over the weir with a non-uniform velocity distribution. Bernoulli equation along an arbitrary streamline A-B can be written with $p_B=0$.

$$\frac{p_A}{\gamma}+\frac{v_1^2}{2g}+Z_A=(h+P-h')+\frac{u_2^2}{2g} \qquad (2.1)$$

Where h′ is the distance from free water surface to the point B.

We do not necessarily need to know the location of point A at section (1) since the total head along the vertical line of section (1) for any particle is constant. Therefore, we can re-write the Bernoulli equation from upstream free water surface to point B at section (2):

$$u_2=\sqrt{2g\left(h'+\frac{v_1^2}{2g}\right)} \qquad (2.2)$$

The flow rate can be calculated from the integration of velocity over the weir opening area:

$$Q=\int u_2 \; dA=\int_{h'=0}^{h'=h} u_2\, w \; dh' \qquad (2.3)$$

Where w=w(h) is the cross-channel width of a strip of weir area. For a rectangular channel W equals b. By substituting u_2 from Eq. (2.2) into Eq. (2.3) flow rate will become:

$$Q = \sqrt{2g}\ b\int_0^h \sqrt{h' + \frac{V_1^2}{2g}}\ \ dh' \qquad (2.4)$$

Integrating Eq. (2.4) will yield Eq. (2.5):

$$Q = \frac{2}{3}\ \sqrt{2g}\ \ b\ \left[\left(h+\frac{V_1^2}{2g}\right)^{\frac{3}{2}} - \left(\frac{V_1^2}{2g}\right)^{\frac{3}{2}}\right] \qquad (2.5)$$

The effect of flow contraction over the weir may be expressed by a contraction coefficient, C_c, leading to the result:

$$Q = \frac{2}{3}\ \sqrt{2g}\, b\, C_c\ h^{\frac{3}{2}}\left[\left(1+\frac{V_1^2}{2gh}\right)^{\frac{3}{2}} - \left(\frac{V_1^2}{2gh}\right)^{\frac{3}{2}}\right] \qquad (2.6)$$

Eq. (2.6) can be expressed in a more compact form by introducing a discharge coefficient, C_d, as:

$$Q = C_d\ \frac{2}{3}\ \sqrt{2g}\ \ b\ h^{\frac{3}{2}} \qquad (2.7)$$

Where:

$$C_d = C_c \left[\left(1 + \frac{V_1^2}{2gh} \right)^{\frac{3}{2}} - \left(\frac{V_1^2}{2gh} \right)^{\frac{3}{2}} \right]$$

The coefficient C_d is termed as discharge coefficient which compensates for all the effects not taken into consideration in derivation of discharge relation. Some of those effects are viscous effects, streamline curvature due to weir contraction, three-dimensional flow structures behind the weir plate and surface tension.

From dimensional analysis arguments, it is found that discharge coefficient is a function of several other parameters.

$$C_d = f(R, W_e, h/b, h/B, h/P) \qquad (2.8)$$

Where R is the Reynolds number, W_e is the Weber number, B is the channel width and P is the weir plate height. In most practical situations the Reynolds number and Weber number effects are negligible and weir geometry is the key element.

CHAPTER 3

LITERITURE REVIEW

3.1. Introduction

A large number of theoretical and experimental researches are conducted on sharp-crested rectangular weirs. The most common objective of those investigations has been to focus on the characteristics of the weirs, among which the discharge coefficient is appearing to be the one representing the hydraulic behavior of the weir.

In this chapter, a brief explanation of earlier studies on discharge coefficient, which are considered to be the most important studies, will be shortly presented. Their findings will be used to make relevant comparisons with the findings of the present study in the following chapters.

3.2. Study of Rehbock, 1929

Rehbock (1929) made one of the earliest experimental studies on C_d (Franzini and Finnemore, 1997). Rehbock (1929) performed experiments on the full width sharp-crested rectangular weirs and found out that discharge coefficient is dependent on the weir height (P) and water head (h). The proposed empirical discharge equation is a function of h over P ratio (h/P).

He conducted experiments on the full width suppressed weirs and for the analytically derived discharge equation (Eq. (2.7)), he proposed the Eq. (3.1):

$$C_d = 0.611 + 0.075\left(\frac{h}{P}\right) + \frac{0.36}{h\sqrt{\frac{\rho g}{\sigma}} - 1} \qquad (3.1)$$

In Eq. (3.1), P is the weir height, ρ is the mass density, σ is the surface tension of the water and h is the water head upstream of the weir plate.

The effect of surface tension can be ignored if h is larger than the head corresponding to the minimum value of C_d. For minima, differentiating C_d with h and equating it to zero would yield the head h_* as:

$$h_* = \sqrt{\frac{\sigma}{\rho g}} + 2.12\left(\frac{\sigma P^2}{\rho g}\right)^{\frac{1}{4}} \qquad (3.2)$$

And if $h > h_*$, then:

$$C_d = 0.611 + 0.08\left(\frac{h}{P}\right) \qquad (3.3)$$

Thus, for $h > h_*$, Eq. (3.1) shrinks to Eq. (3.3) which does not reflect the viscous and surface tension effects, but rather it is merely a function of weir geometry.

Rehbock's C_d relation has been observed to be precise for values of P ranging from 0.1 to 1 m. Also, for the value of h changing from 0.025 to 0.6 m and for the ratios of h/P not any greater than 1.

3.3. Study of Kindsvater and Carter, 1957

Kindsvater and Carter (1957), by taking the viscous and surface tension effects into account, presented a concept which would correct the head and weir width in order to compensate the mentioned effects (Strum, 2001).

Based on experimental results collected at Georgia Institute of Technology, Kindsvater and Carter (1957) found that Reynolds number and Weber number effects can be added to the head-discharge relationship by making slight corrections to the head (h) and the crest length (b). By doing so, they derived an effective discharge coefficient, C_{de}, which depended only on h/P and b/B. Their relationship is given in the form of an equation:

$$Q = C_{de} \frac{2}{3} \sqrt{2g}\ b_e\ h_e^{\frac{3}{2}} \quad (3.4)$$

In which:

$$b_e = b + K_b \quad (3.5)$$

$$h_e = h + K_h \quad (3.6)$$

Where b_e is effective weir width, h_e is effective water head, the values of C_{de} and K_b are given in Figures 3.1 and 3.2, respectively. K_h was found to be nearly constant with an approximate value of 0.001 m for all b/B ratios.

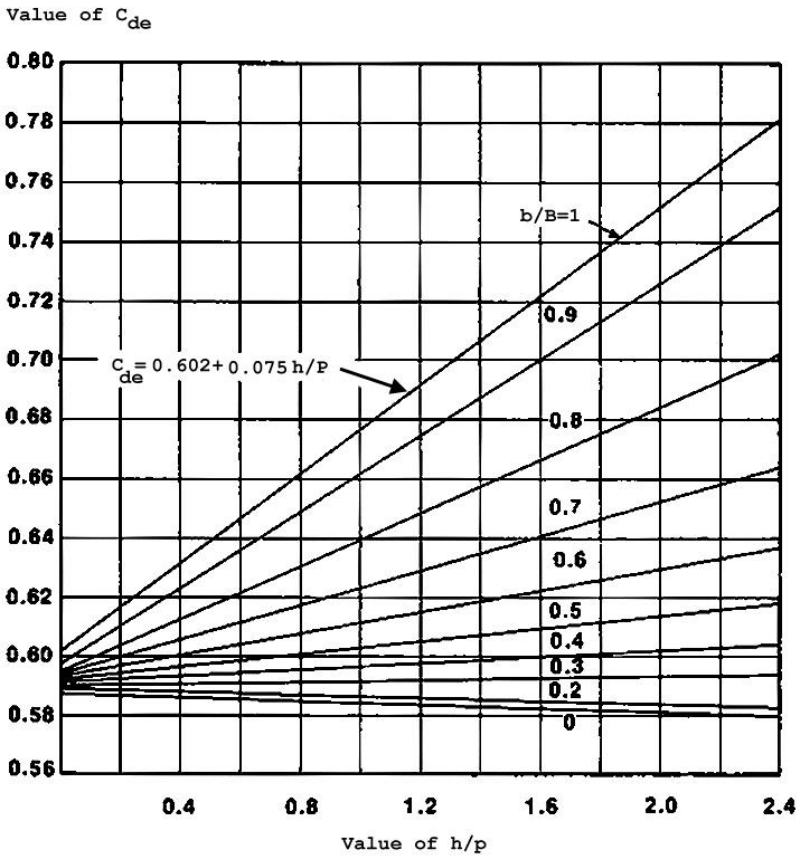

Figure 3.1 Coefficient of discharge (Sturm, 2001)

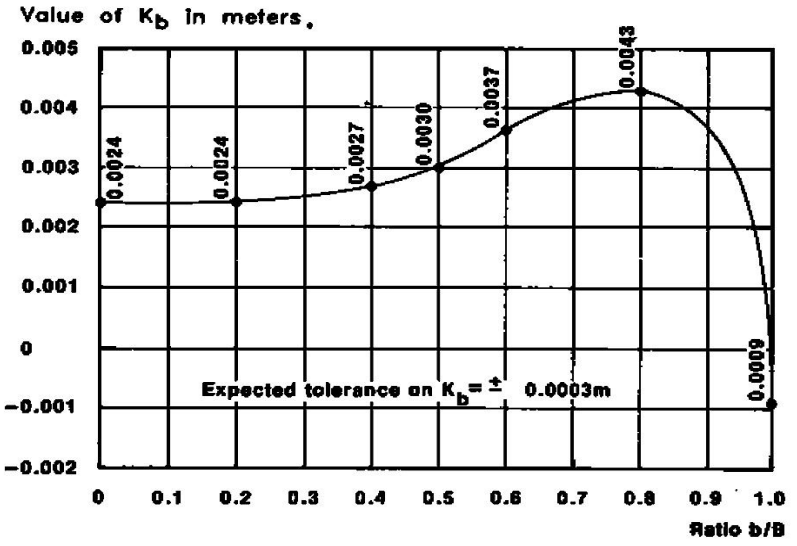

Figure 3.2 Crest Length Corrections (Sturm, 2001)

K_b is maximum at b/B=0.8 with a value of 0.0043 m, as it is shown in Figure 3.2. Equations for C_{de} are given as a function of the lateral contraction ratio of (b/B) and the vertical contraction ratio, (h/P), in Table 3.1 Kindsvater and Carter found that there was little influence of (h/P) on the discharge coefficient.

Kindsvater and Carter (1957) constructed their sharp-crested weir notches, not with a very sharp edge but with an upstream square edge having a top width of 1.3 mm and a downstream bevel. For exact measurements, Kindsvater and Carter (1957) suggested a limitation of h/P<2, with P no less than 9 cm. If h/P exceeds 5, the weir section will no longer remain as the control section and for that reason such values should be avoided.

Table 3.1 Discharge coefficients for the Kindsvater & Carter formula (Sturm, 2001)

b/B	C_{de}
1.0	0.602+0.075(h/P)
0.9	0.599+0.064(h/P)
0.8	0.597+0.045(h/P)
0.7	0.595+0.03(h/P)
0.6	0.593+0.018(h/P)
0.5	0.592+0.011(h/P)
0.4	0.591+0.0058(h/P)
0.3	0.590+0.002(h/P)
0.2	0.589-0.0018(h/P)
0.1	0.588-0.0021(h/P)
0.0	0.587-0.0023(h/P)

3.4. Study of Kandaswamy and Rouse, 1957

Kandaswamy and Rouse (1957) experimentally investigated the discharge coefficient, where their results were divided into two separate ranges of (h/P) ratios ($h/P \leq 5$, $h/P \geq 15$)(Chow, V. T., 1959). They found that for values of h/P up to 5, Rehbock's (1929) formula of discharge coefficient works properly and it could be used for h/P values extended to up 10 with fair approximation. For h/P greater than 15, weir acts as sill and weir section becomes a control. For the mentioned range they suggested a simple function for discharge coefficient as a function of h/P ratio. Their findings do not clearly define the behavior of weir for the range of $10 \leq h/P \leq 15$.

3.5. Study of Ramamurthy et al., 1987

Ramamurthy et al. (1987), based on theoretically simplified momentum principle and experimental derivation of pressure distribution at weir face and momentum coefficients, found that discharge coefficient (C_d) for flow over a sharp-crested weir is semi-empirically related with h/P ratio, where weir range is $0 \leq h/P \leq 10$ and sill range is $10 \leq P/h \leq \infty$. The general C_d relation proposed was examined to be in close agreement with earlier studies.

3.6. Study of Swamee, 1988

Swamee (1988) suggested a full-range weir equation, Eq. (3.7), by combining Rehbock (1929) and Rouse (1963) proposed equations and fitting the experimental data of Kandswamy and Rouse (1957). The given equation would hold good for extreme variations of head over weir height ratios (h/P). The proposed equation can be applied to sharp-crested, narrow-crested, broad-crested and long-crested weirs.

$$C_d=1.06\left\{\left(\frac{14.14P}{8.15P+h}\right)^{10}+\left(\frac{h}{h+P}\right)^{15}+1.834\left[1+0.2\left(\frac{\left(\frac{h}{L}\right)^{5}+1500\left(\frac{h}{L}\right)^{13}}{1+1000\left(\frac{h}{L}\right)^{3}}\right)^{0.1}\right]^{-10}\right\}^{-0.1} \quad (3.7)$$

3.7. Study of Aydin et al., 2002

Aydin et al. (2002) came up with the idea of a slit weir used for measuring small discharges. They found a discharge coefficient in terms of Reynolds number. In 2006, the proposed relation was improved by introducing the non-dimensional term h/b along with utilizing Reynolds number in the formulation of discharge coefficient.

A rectangular slit weir is designed to measure small discharges. The discharge coefficient they determined is empirically derived from experiments. All relevant relationships between dimensionless parameters and discharge coefficient were also investigated. It was

eventually discovered that the discharge coefficient is solely a function of Reynolds number for the certain range they recommended.

$$C_d = 0.562 + 11.354/R^{0.5} \qquad (3.8)$$

The collected data was substituted in the discharge equation, Eq. (2 .7), and the values of C_d were found for those data. Once the values of C_d were determined, they plotted the data against the Reynolds number as shown in Figure 3.3. The best fit expression was also searched and Eq. (3.8) was suggested.

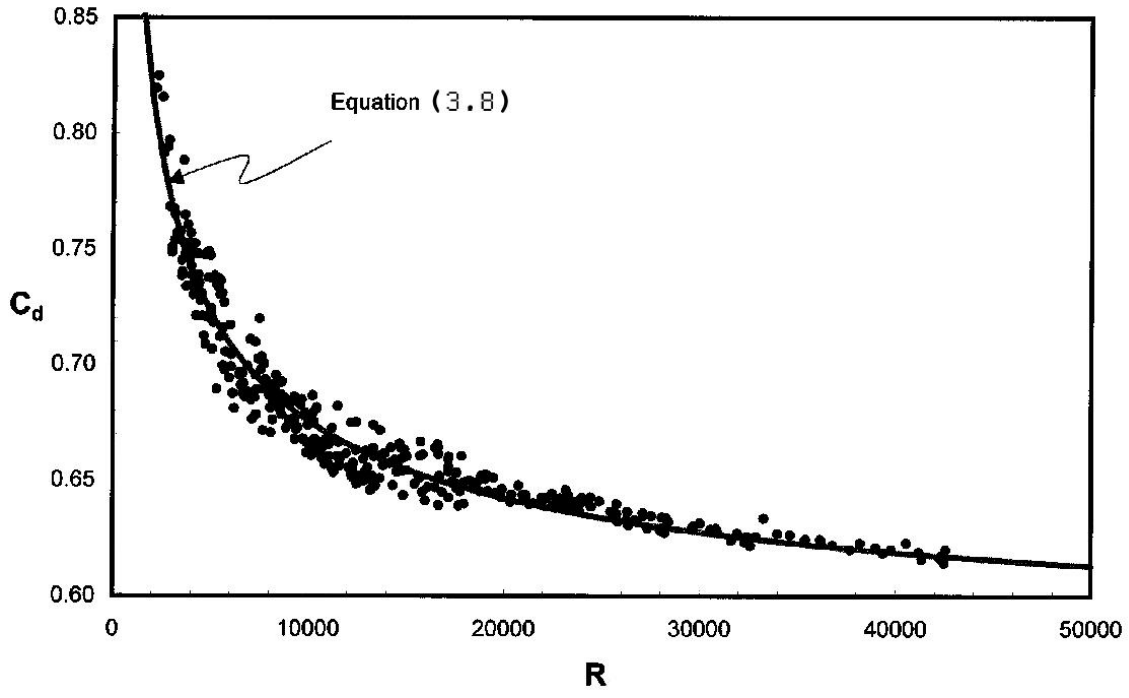

Figure 3.3 Discharge coefficient data (Aydin et al., 2002)

Using slit weir will significantly increase the precision of discharge measurement. If the term dQ/dh is considered as the precision, change in head per unit change in discharge, accuracy of the slit weir is much higher than that of partially contracted or triangular weirs.

The root mean square error in obtaining discharge using Eq. (3.8) is 0.0096 (l/s). As shown in Figure 3.3, 5.8% of the data falls within the ±1% of the value predicted by Eq. (3.8). For very small values of h/b and or h/B such that $h^2/Bb < 0.2$, the validity of the assumptions made in formula may be questionable. Therefore, when $h^2/Bb < 0.2$, suggested formula should not be used in determining the discharge coefficient. In addition, for b<0.005 m, the influence of surface tension is dominant and using the Eq. (3.8) would yield wrong predictions of discharge and is not recommended to use the formula for these ranges.

3.8. Study of Aydin et al., 2006

This study was in consistency with the findings of the previous research (Aydin et al., 2002). The slit weirs were more closely investigated and an improved relation for discharge coefficient as a function of Reynolds number was determined.

For a slit weir, channel width should be large enough so that the approach velocity head can be ignored. The upper bound to dismiss the channel width effect was suggested to be $b/B \leq 1/4$.

In their studies, they concluded that at least two dimensionless parameters are required in definition of C_d to cover the full measuring range. After performing regression analysis of the data, they found that Reynolds number and h/b can better represent the discharge coefficient.

$$C_d = 0.562 + \frac{10\left\{1-\exp\left[-\left(\frac{2h}{b}\right)^2\right]\right\}^{-1}}{R^{0.45}} \qquad (3.9)$$

For h/b > 2, they defined a best fit relation for C_d :

$$C_d = 0.562 + \frac{10}{R^{0.45}} \qquad (3.10)$$

The relative error is within ±2% for 89% of the entire experimental data. The relative error reduces as the measured discharge increases.

3.9. Study of Ramamurthy et al., 2007

Ramamurthy et al. (2007) introduced the concept of a "multislit weir". The multislit weir is a combination of several single slit weirs. It is used to measure both small

and large discharges with high accuracy. In their extensive investigation, they used three different multislit weir units (n=3, 7 and 15) and the weir opening of 5 mm. They concluded that for small Reynolds numbers, the discharge coefficient is mainly dependent on Reynolds number, whereas this dependency decreases as the Reynolds value increases. In large Reynolds numbers "Inertia forces are high and viscous forces are negligible" therefore C_d is less affected by the Reynolds number.

3.10. Study of Bagheri and Heidarpour, 2010

Bagheri and Heidarpour (2010) developed an expression for C_d in sharp-crested rectangular weirs which was based on free-vortex theory. In their experimental investigation they obtained a relation for upper and lower nappe profiles, a two and three-degree polynomial were found for each as the best fit representatives, respectively. They used the obtained profile equations in the potential flow theory in order to integrate the velocity of free-vortex motion between upper and lower nappe, in the section where flow is assumed to be potential. They defined the discharge coefficient in terms of the dimensionless terms b/B and h/P as Eq. (3.11):

$$C_d = 0.324 \exp\left[0.94\left(\frac{b}{B}\right)\right] \ln\left[1+\frac{0.73\left(\frac{h}{P}\right)+3.64}{\exp\left(1.18\frac{b}{B}\right)}\right] \qquad (3.11)$$

The best fit approximation they achieved for C_d is valid for the range $0<h/P<9$ and outside the recommended range, C_d starts to drift away from actual data records.

3.11. Study of Aydin et al., 2011

Aydin et al. (2011) introduced the concept of average weir velocity. According to their study using weir velocity instead of discharge coefficient can lead to a more realistic and accurate measurement of discharge in rectangular weirs. Since weir velocity has a universal distribution pattern, discharge can better be formulated in terms of average weir velocity which can easily be fit empirically. They also divided the weirs into two categories, partially and fully contracted (slit) weirs. Partially contracted weirs cover the range of $0.25 \leq b/B \leq 1$ and slit weirs fall in the range of $b/B \leq 0.25$.

Their experimental investigation focused on the applicability of various formulations of discharge relation to free it from discharge coefficient. They introduced the weir velocity term:

$$V_w = \frac{Q}{bh} \qquad (3.12)$$

Plotting weir velocity against the weir head illustrates a universal behavior which can be used in a way that can express a relationship for discharge formula. In addition,

according to the same plots, it can be realized that the curves have a unique appearance from best fit point of view. As an initial assumption, they expressed the weir velocity as:

$$V_{wc} = c_1+c_2h+c_3h^{1.5} \quad (3.13)$$

$$V_{ws} = d_1+d_2h+d_3h^{1.5} \quad (3.14)$$

Where, V_{wc} is the contracted weir velocity and V_{ws} is slit weir velocity.

Unknown coefficients in the Eq. (3.13) and (3.14) were obtained by a multivariate optimization approach. For the partially contracted weir range the following coefficients were determined as:

$$c_1 = 0.252-0.068(b/B)+0.002(b/B)^2 \quad (3.15)$$

$$c_2 = 3.937+0.760(b/B)+2.426(b/B)^2 \quad (3.16)$$

$$c_3 = -2.238-2.856(b/B)-1.427(b/B)^2 \quad (3.17)$$

And similarly for the slit weir case:

$$d_1 = 0.268-0.7882(b/B)+2.474(b/B)^2 \quad (3.18)$$

$$d_2 = 5.650-1.376(b/B)-10.879(b/B)^2 \quad (3.19)$$

$$d_3 = -5.159+0.336(b/B)+22.741(b/B)^2 \quad (3.20)$$

3.12. Conclusion

As mentioned earlier, because of complicated nature of weir, it is not easy to analytically find a discharge equation which can represent the actual behavior of the weir. Therefore, many investigators have tried to combine empirical and analytical approaches to develop an expression that can calculate the discharges over the weirs accurately.

In order to be able to explain contributions of the present study to the previous ones, experimental findings of the present study will be compared to the results of the earlier studies in relevant occasions. Also, percent difference between the present and previous studies will be given in the 5^{th} Chapter.

CHAPTER 4

EXPERIMENTAL SETUP AND PROCEDURES

4.1. Experimental setup

The experimental setup consists of a 6 m long rectangular channel with a width of 0.32 m and a depth of 0.70 m and it is made up of Plexiglas. There is a tank underneath the channel exit where water is released into. Its cross-sectional area is 1 m^2. Water is supplied from upstream entrance through a pipe with a diameter of 0.20 m (Figure 4.1).

Figure 4.1 Experimental setup

The discharge in the channel is controlled by a valve before it reaches the entrance tank. At the end of the entrance tank there are several vertical parallel screens which are meant to subside the fluctuations generated at the water surface. In spite of screens' existence, in large heads usually stationary waves developed, therefore, a wooden floating plate was installed upstream of the screens to counteract the effect and regulate the flow (Figure 4.2).

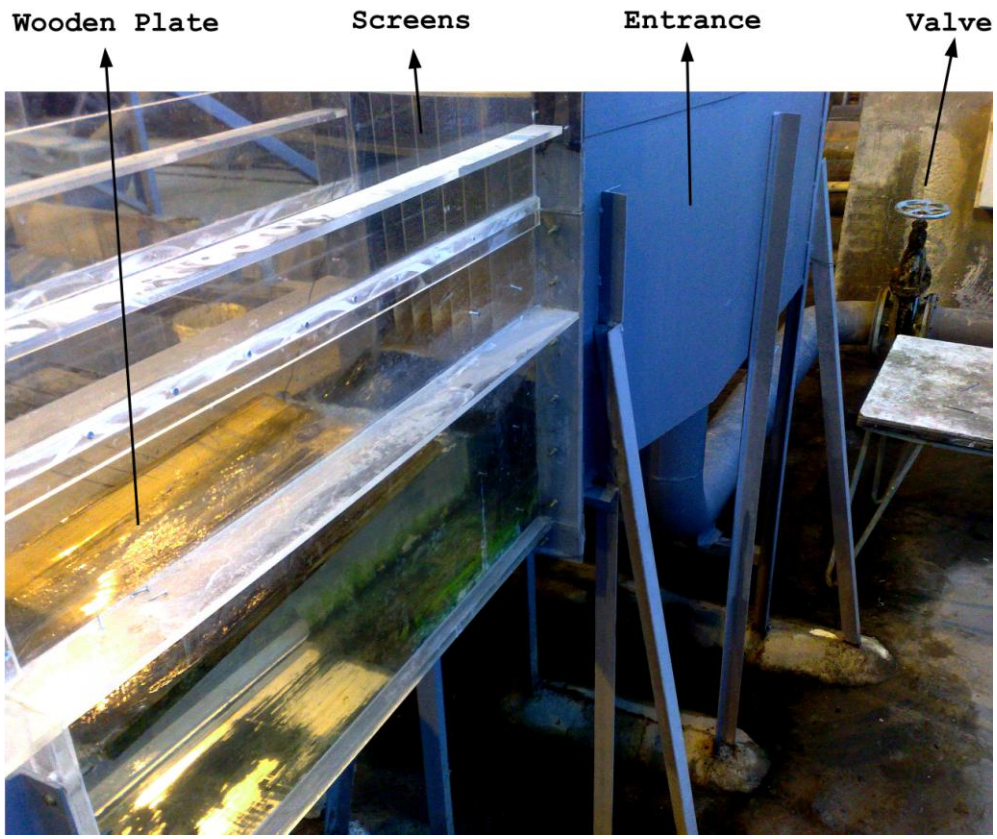

Figure 4.2 Entrance Components

After the entrance, water passes through a rectangular channel and exits over the weir down into the tank and this circulation continues. Water head is measured at a distance of 2.2 m upstream of the weir section. In literature, it is recommended that 3-4 times the maximum water head will be far enough to get rid of the water drawdown while approaching the exit section (Bos, 1989). In our case maximum head recorded was around 0.54 m, thus 4 times 0.54 m will equal 2.16 m which is acceptable. A point gauge is used to measure the water head at the centerline of the approach channel. Its accuracy is 0.1 mm (Figure 4.3).

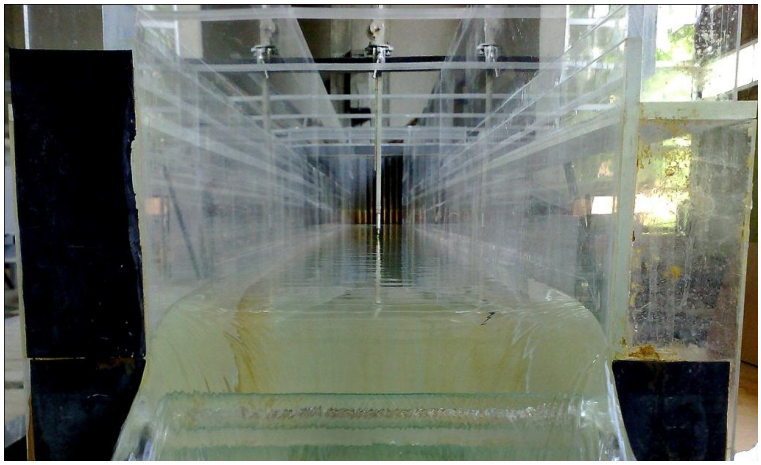

Figure 4.3 View of the point gauge

For constructing the contraction in the weir, two pieces of Plexiglas sheets were used. By adjusting the distance of opening gap between the plates, the desired contraction width was obtained and the surrounding of the plates were insulated against the unwanted leakages (Figure 4.4).

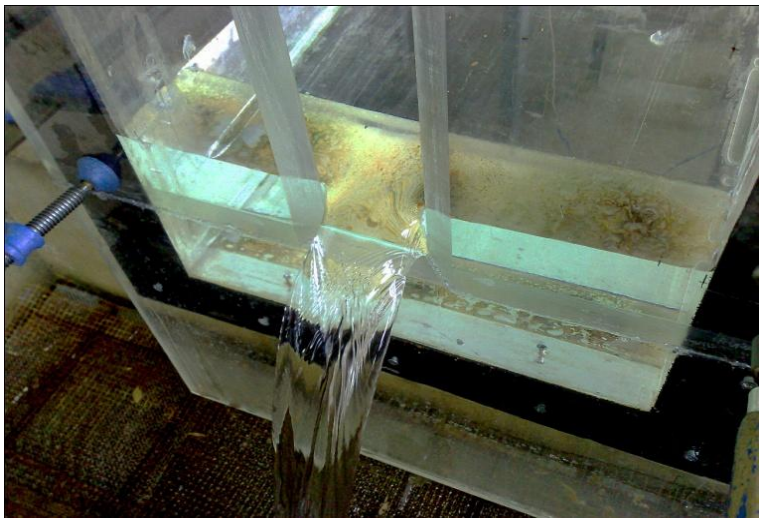

Figure 4.4 Plexiglas sheets and weir

Figures 4.5 and 4.6 show the schematic plan view and side view of the setup, respectively.

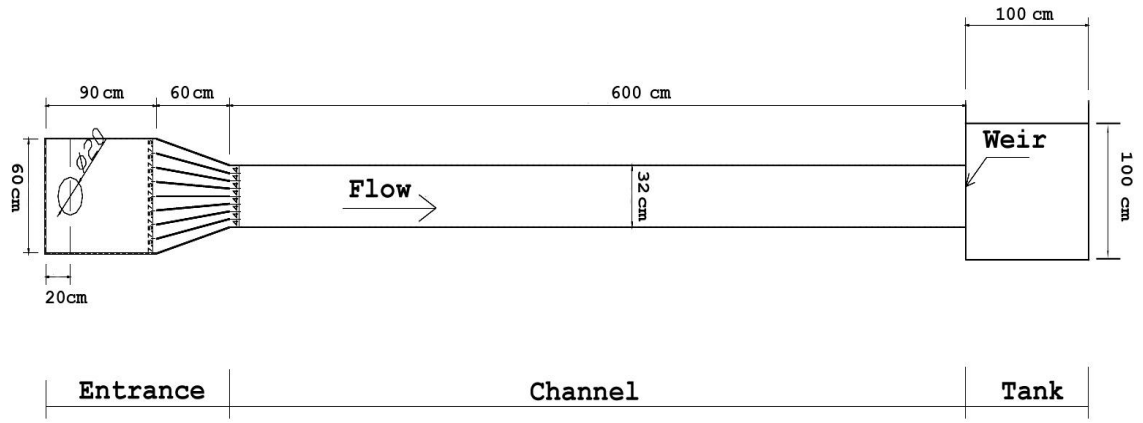

Figure 4.5 Schematic plan view of the setup

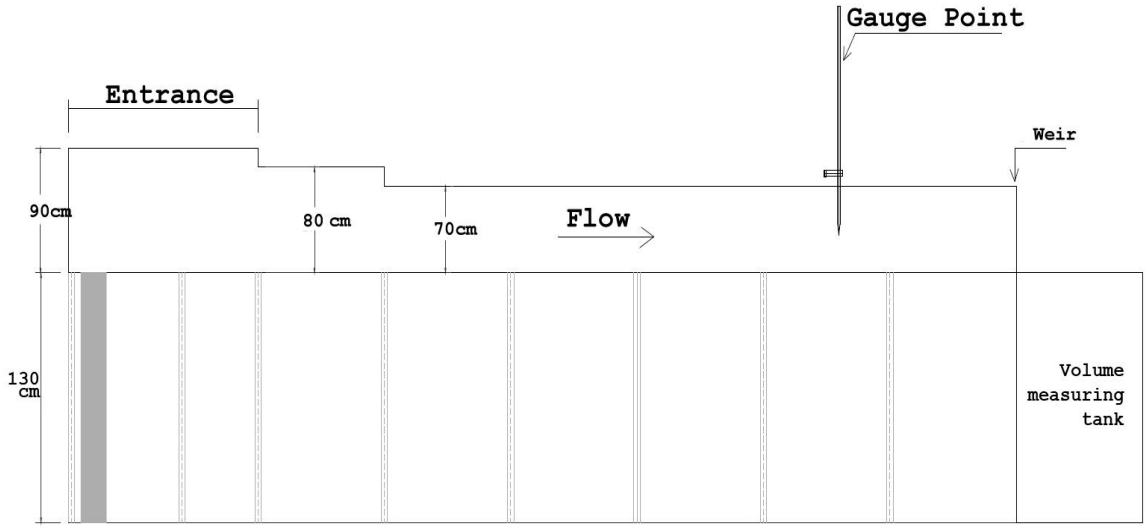

Figure 4.6 Schematic side view of the setup

4.2 Pressure Transducer, Amplifier and Digitizer

For discharge measurement, gate under the tank exit is kept closed such that water can accumulate in the tank. Since the area of the tank (from plan view) is equal to 1 m^2, if the velocity of the rising water is measured, discharge of the stream will be calculated using Eq. (4.1).

$$Q = V.A \qquad (4.1)$$

In which: V is the velocity of the rising water surface and A is the cross-sectional area of the tank (A=1 m^2).

In order to measure the mentioned velocity, several electronic devices are used. Firstly, it is the pressure transducer (Figure 4.7) which senses the pressure rise due to water rise in the tank and sends the corresponding signals to the amplifier (Figure 4.8). Amplifier magnifies the received signals from transducer and transmits them to the digitizer (Figure 4.8). Digitizer takes care of the final stage, converts the analog signals to digital values and delivers them to the computer. It is essential to calibrate the digitizer before calculating the discharge. In order to calibrate the digitizer, initially by multiplying the voltage with a constant, voltage should be converted into water depth. For this purpose in several measurements, constant water depth in the tank and a corresponding voltage is recorded, by plotting the water depth against the voltage, a best fit line is drawn amongst the points, calibration constant is the slope of that line.

Figure 4.7 Pressure Transducer

Figure 4.8 Amplifier & Digitizer (small white device)

Once the data collected from digitizer are stored in the computer, velocity will be computed from plots of calibrated data. For this purpose, recorded voltage values are converted into water depths by multiplying them with the calibration constant. Then the data pairs- time and water depth- are plotted in a proper computer software and a best fit line is drawn. The line will have a constant slope which is the velocity of rising water in the tank (Figure 4.9).

Figure 4.9 is showing one typical graph for discharge measurement. By entering the data points into the graph and applying a best fit line, the slope of the line will demonstrate the velocity of the water rise in the tank.

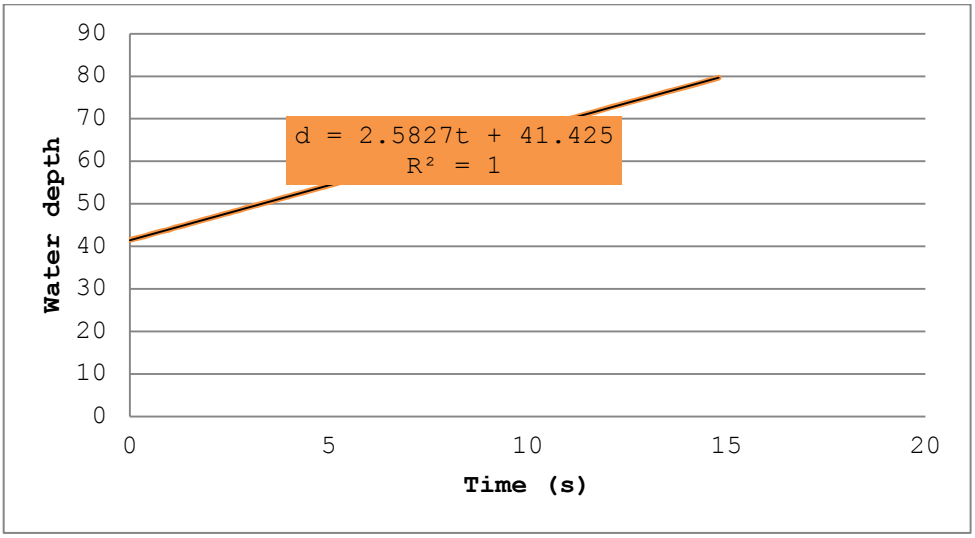

Figure 4.9 A typical graph for water depth versus time

CHAPTER 5

RESULTS AND DISCUSSIONS

5.1. Introduction

In this chapter, results of the experiments are discussed and comparisons between the measured data and the results given by earlier studies are made.

In the Section 5.1.1, measurements on different weir heights are presented and a constant value for P (weir height) is chosen to continue the rest of the experiments. The height for which, bottom boundary layer effects on the flow are minimized. In the following section (Section 5.1.2), experiments for different weir openings will be shown. Later on, in Section 5.2, distinguishing the slit from contracted weirs will be argued. In Section 5.2.1 to 5.2.3, comparisons of the collected data with the previous works are discussed in detail. Finally, in Section 5.3 and 5.3.1 results and ideas original to this research are offered.

In another different attempt, adaptability of the Dressler theory to the weir flow was inspected. But since the objectives of the study faced several hurdles, and sophisticated techniques may be required to successfully chase the goals of the research, no offerable result was achieved to demonstrate. Nevertheless, experimental data and some details of the mentioned activity are elucidated in Section 5.4.

5.1.1. Experiments on Different Weir Heights

In this research, after performing a number of experiments on different weir heights, a constant height was selected in order to continue the rest of experiments accordingly. By changing the weir height(P=2, 4, 6, 8, 10, 13, 16, 19, 22, 25 cm) and observing discharge variation with respect to water head, as indicated in Figure 5.1, it was found that weir height has little influence on the discharge for values of P greater than 10 cm for the discharge range covered in the present study. Therefore, it was concluded that weir height value ought to be kept fixed at 10 cm to prevent boundary layer development- this value is suggested by Bos (1989) too. Thus, any P greater than the recommended value will hydraulically imply that the flow over the weir is no longer relying on the weir height. In addition, it is realizable that the chosen P may remain valid for the experimental range of water head recordings only. Once the range is violated, it can be expected that larger weir

plate heights might be required to suppress boundary layer development.

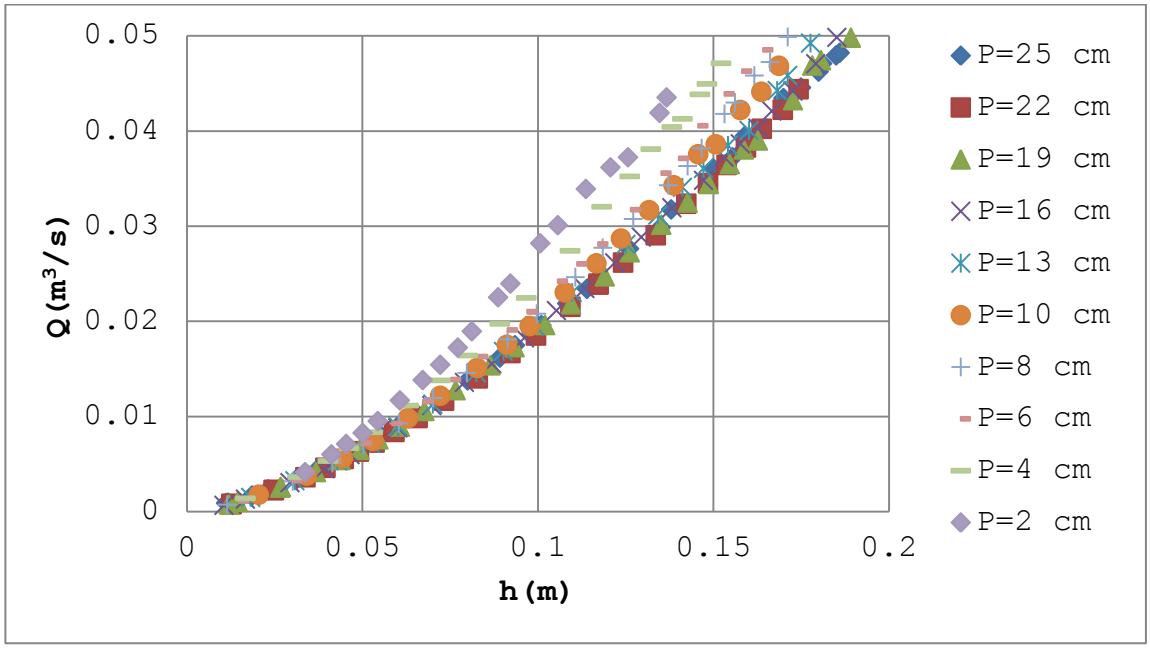

Figure 5.1 Discharge & water head relation for various weir heights

It is worth mentioning that the P selection was based on full width weir case (the condition in which b=B), contracting the weir section from either sides will further reduce the average velocity in the approach channel and therefore suppress the boundary layer growth.

5.1.2. Experiments on Different Weir Openings

Once the weir height was decided to be kept at 10 cm, experiments continued with different weir openings. There were 21 different weir openings tested in this study (b = 1, 2, 3, 4, 5, 6, 7, 8, 9, 10, 12, 14, 16, 18, 20, 22, 24, 26, 28, 30, 32 cm) and 394 data points were collected in total in the laboratory. Figure 5.2 shows the whole data points, discharges at different water heads for different weir openings (b). Large discharges were more difficult to measure in the laboratory and this can be seen in Figure 5.2 (For b18 and b32 for example, there are some outlying points, detectable among other outliers), this difficulty is due to the fact that for large heads of water, stationary waves form on the water surface, resulting in either head recording mistakes or mistakes in measuring discharge itself.

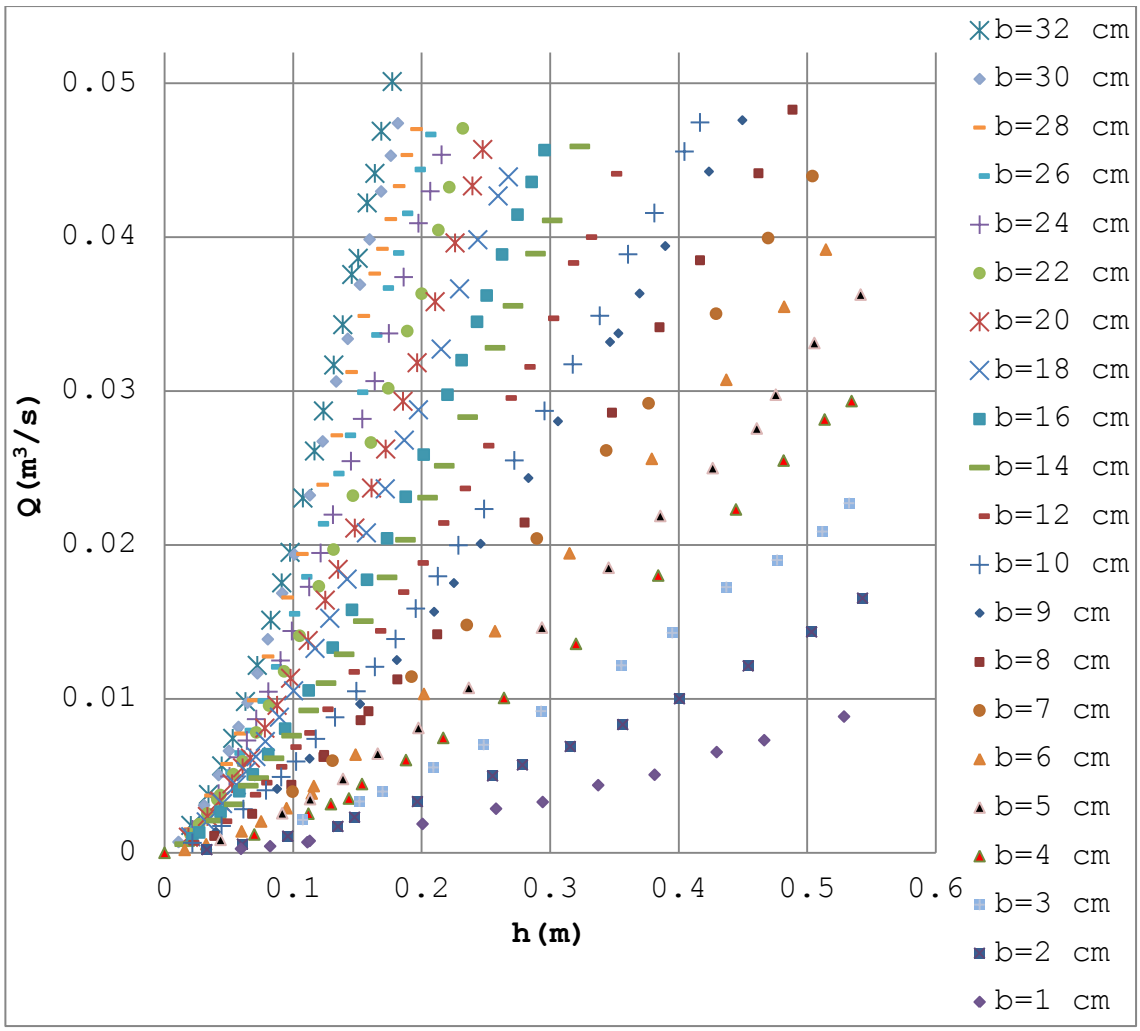

Figure 5.2 Discharge and water head data for different weir widths

In Table 5.1, experimental data range is displayed. Water head is roughly enclosed between 1 cm and 54 cm which covers a wide spectrum of different discharges starting from 0.00026(m^3/s) to 0.0501(m^3/s). Discharges corresponding to heads smaller than 1 cm were avoided since this could lead to aeration problem (When water clings to the weir

plate in small discharges, aeration stops and no nappe takes place in front of the weir).

Table 5.1 Experimental study spectrum

b (m)	P (m)	Q_{min} (m^3/s)	Q_{max} (m^3/s)	h_{min} (m)	h_{max} (m)	$(h/b)_{min}$	$(h/b)_{max}$	$(h/P)_{min}$	$(h/P)_{max}$	b/B
0.01	0.1	0.00026	0.00885	0.0595	0.5288	5.95	52.88	0.595	5.288	0.03125
0.02	0.1	0.000205	0.016544	0.033	0.5432	1.65	27.16	0.33	5.432	0.0625
0.03	0.1	0.00213	0.02271	0.1077	0.5327	3.59	17.75667	1.077	5.327	0.09375
0.04	0.1	0.00119	0.02934	0.0699	0.5347	1.7475	13.3675	0.699	5.347	0.125
0.05	0.1	0.00084	0.0362	0.0436	0.5417	0.872	10.834	0.436	5.417	0.15625
0.06	0.1	0.00019	0.039182	0.0157	0.5147	0.261667	8.578333	0.157	5.147	0.1875
0.07	0.1	0.000158	0.045048	0.0115	0.5267	0.164286	7.524286	0.115	5.267	0.21875
0.08	0.1	0.000818	0.046151	0.0317	0.4727	0.39625	5.90875	0.317	4.727	0.25
0.09	0.1	0.00136	0.04759	0.04	0.4497	0.444444	4.996667	0.4	4.497	0.28125
0.1	0.1	0.000643	0.047448	0.0217	0.4167	0.217	4.167	0.217	4.167	0.3125
0.12	0.1	0.00065	0.04411	0.0192	0.3482	0.16	2.901667	0.192	3.482	0.375
0.14	0.1	0.00056	0.045886	0.0157	0.3232	0.112143	2.308571	0.157	3.232	0.4375
0.16	0.1	0.000942	0.045649	0.0217	0.2957	0.135625	1.848125	0.217	2.957	0.5
0.18	0.1	0.001043	0.043909	0.0204	0.2676	0.113333	1.486667	0.204	2.676	0.5625
0.2	0.1	0.00101	0.04569	0.0186	0.2476	0.093	1.238	0.186	2.476	0.625
0.22	0.1	0.001217	0.047062	0.0201	0.2321	0.091364	1.055	0.201	2.321	0.6875
0.24	0.1	0.001521	0.045344	0.0218	0.2156	0.090833	0.898333	0.218	2.156	0.75
0.26	0.1	0.001616	0.046665	0.0206	0.2036	0.079231	0.783077	0.206	2.036	0.8125
0.28	0.1	0.001525	0.047015	0.0196	0.1961	0.07	0.700357	0.196	1.961	0.875
0.3	0.1	0.000705	0.047393	0.0109	0.1816	0.036333	0.605333	0.109	1.816	0.9375
0.32	0.1	0.001782	0.050101	0.0205	0.1772	0.064063	0.55375	0.205	1.772	1

5.2. Slit and Contracted Weirs

As mentioned before in the Chapter 3, literature review, Aydin et al.(2002) suggested that for the slit weirs, b/B should be less than 0.25 in order to ignore the approach velocity head in the channel. Later on, in 2011, they came up with the concept of the weir velocity. Based on the weir velocity's trend shift observed when plotted against available head, it was once more demonstrated that b/B may be ¼ times the channel width which confirmed the previous findings. The mentioned value was proposed as the boundary between slit and contracted weirs.

In the present study, which is fundamentally developed by framing the data analysis into weir velocity, finding the separating b/B ratio was not so firmly identified. Still, by looking at Figure 5.3, it could be explained that the dividing b/B ratio may be assumed as around 0.3. Selection of this point will be discussed in detail in the following paragraph and following sections.

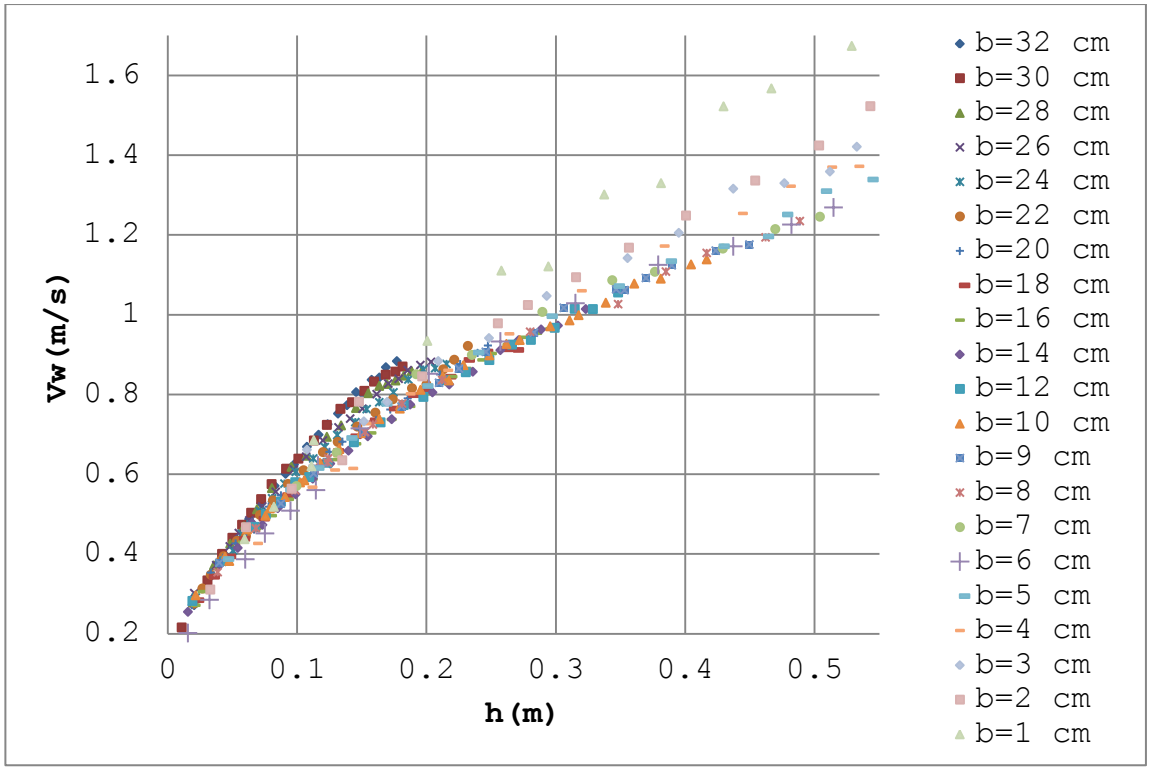

Figure 5.3 Weir velocity for all weir openings

In Figure 5.3, weir velocity initially starts to generally diminish, beginning from b=32 cm to around b=14 cm, after that no trend changes can be recognized up to b=7 cm, in other words, all of the weir velocities corresponding to the range of 7cm ≤b≤ 14cm, are more or less overlapping. Starting from b=1 cm to b=7 cm, there is a clear increasing trend in weir velocity. With all these in mind, it is noticeable that there may exist a transition zone in 7cm ≤b≤ 14cm. In the transition zone, almost all of the weir velocity curves are overlapping with random ups and downs which originate from experimental error. Taking the middle b as the turning point, b/B ratio is obtained as 0.32. So,

the boundary separating b/B ratio might be revolving around that value (Decision on a selecting b/B=0.3 ratio is discussed in Section 5.3).

This value (b/B=0.3) will be used afterwards to progress the comparing of the present data with the previous studies in the following sections of this chapter. So, a sharp crested rectangular weir having an opening width of less than 0.3B would be assumed as (fully contracted) slit weir and outside the mentioned range, it would be called as(partially)contracted weir.

Figures 5.4, 5.5 and 5.6 represent the variation of experimental discharge coefficient (C_d, which is calculated by Eq. (2.7)) with Reynolds number, Weber number and h/b ratio, respectively.

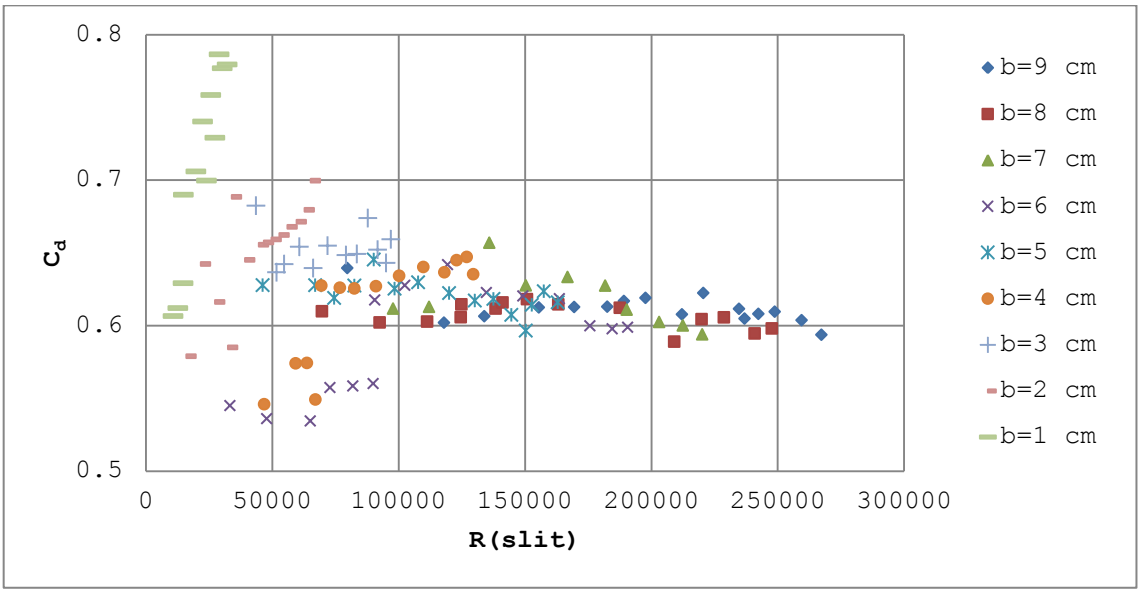

Figure 5.4 C_d versus Reynolds number for slit weirs

Reynolds number for slit weirs is given by Eq. (5.1) (Aydin et al., 2006):

$$R_{slit} = \frac{b\sqrt{2gh}}{\nu} \quad (5.1)$$

In which $\sqrt{2gh}$ is the Torricelli velocity or characteristic velocity, b is the length parameter and ν is kinematic viscosity of the fluid.

On the other hand, in contracted weirs, an improved Reynolds number is used. Square root of the flow area at the weir section is chosen as the characteristic length parameter and that is because in contracted weirs, both the head and the width of the weir are important. The Reynolds number for contracted weirs is given by the Eq. (5.2):

$$R_{contracted} = \frac{\sqrt{bh}\sqrt{2gh}}{\nu} \quad (5.2)$$

Where, $\sqrt{bh}$ is the characteristic length.

In Figure 5.5, variation of discharge coefficient with Weber number is given. Weber number is given as in Eq. (5.3).

$$W_e = \frac{\rho b\left(\sqrt{2gh}\right)^2}{\sigma} = \frac{2ghb\rho}{\sigma} \quad (5.3)$$

In which, $\sqrt{2gh}$ is the Torricelli velocity, b is the characteristic length. ρ is the fluid density and σ is surface tension.

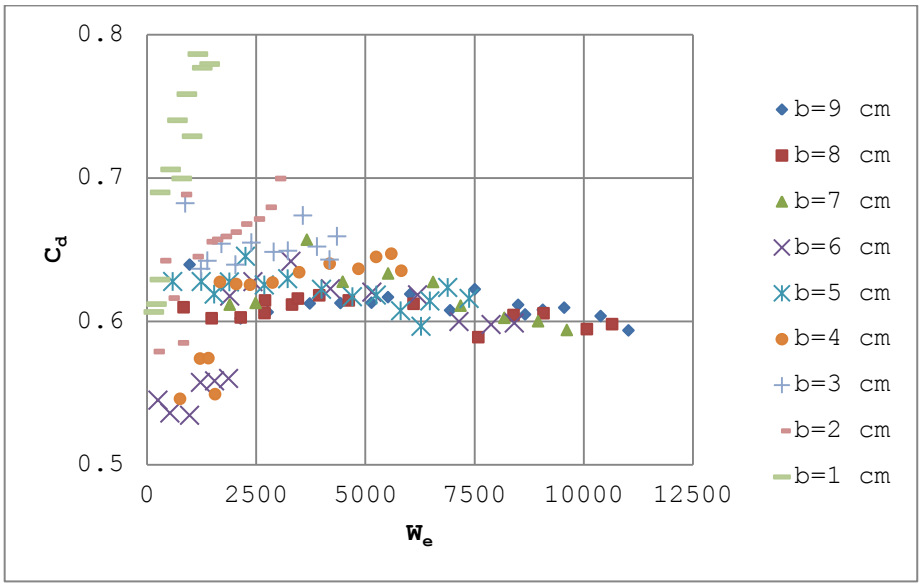

Figure 5.5 C_d versus Weber number for slit weirs

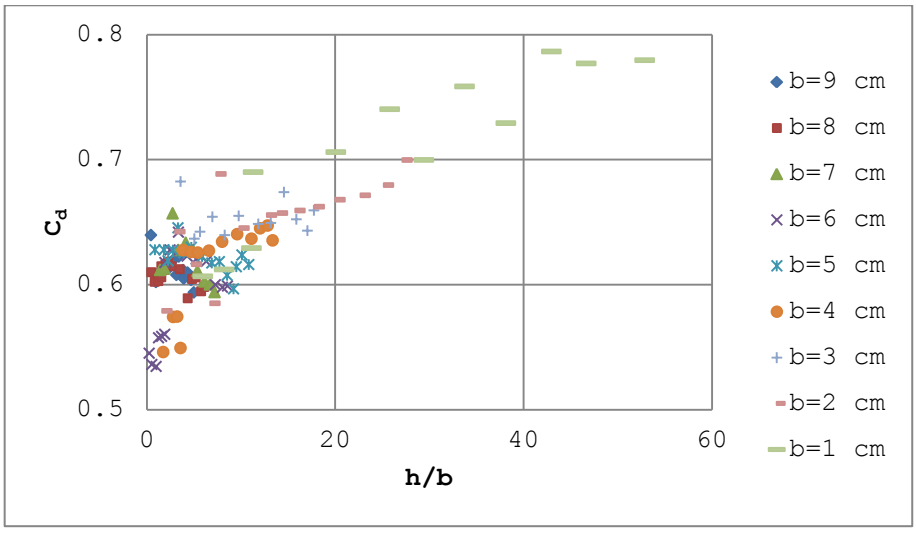

Figure 5.6 C_d versus h/b for slit weirs

5.2.1. Slit weir case comparison with Kindsvater and Carter, 1957

In Figure 5.7, experimental data is compared with the discharge obtained by Kindsvater and Carter's (1957) Equation presented in Section 3.3.

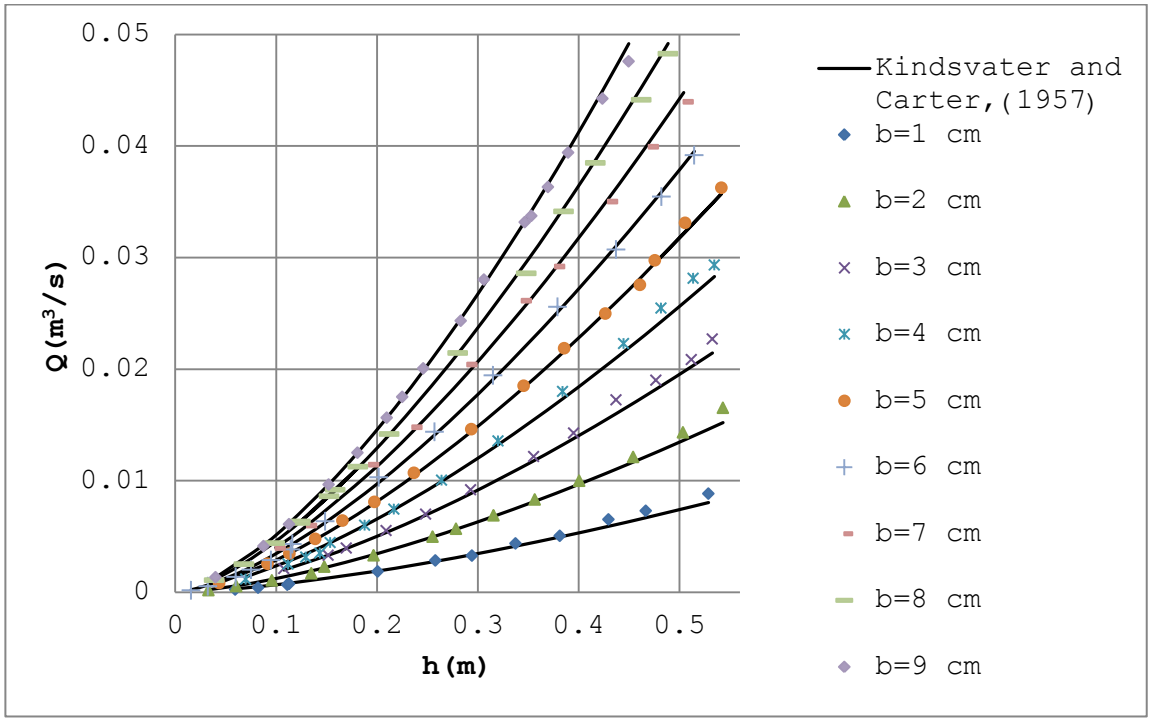

Figure 5.7 Comparison of slit weir data with Kindsvater and Carter's Equation

Even though Kindsvater and Carter's limitations of the slit weir expressions are in some of the cases violated in the present comparison, but the overall matching is not so harshly effected by them. The average error percentage for the difference between the experimental and the expression-given discharges is 3.96 percent (Absolute value).

The differences between the measured and calculated discharges are illustrated in Figure 5.8. The error calculation function is presented in Eq. (5.4).

$$\% \text{ Error} = \frac{Q_{exp} - Q_{calc}}{Q_{exp}} \times 100 \qquad (5.4)$$

In which:

Q_{exp} is the experimentally measured discharges

Q_{calc} is the discharges calculated through the Eq. (3.4)

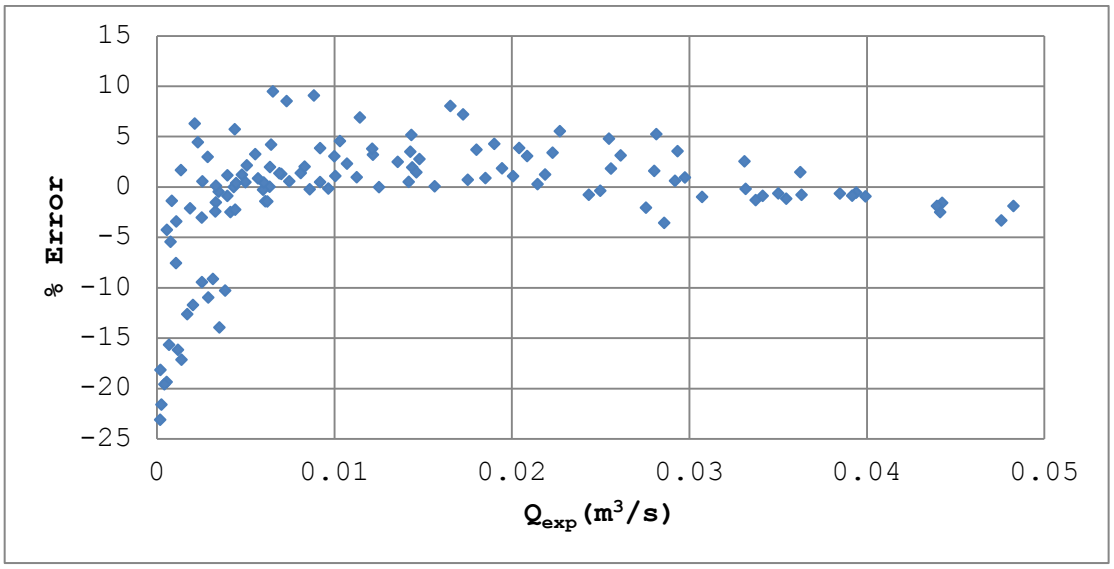

Figure 5.8 Percent error with respect to experimental discharge and Eq. (3.4)

The reason for large errors in small discharges in Figure 5.8 could be that the Kindsvater and Carter (1957) formula has not been suggested for the range h>0.07 cm, whereas there are a couple of measurements for that range in the experimental data.

5.2.2. Slit Weir Case Comparison with Aydin et al., 2006

The experimental data are compared with the study of Aydin et al.(2006) in Figure 5.9.

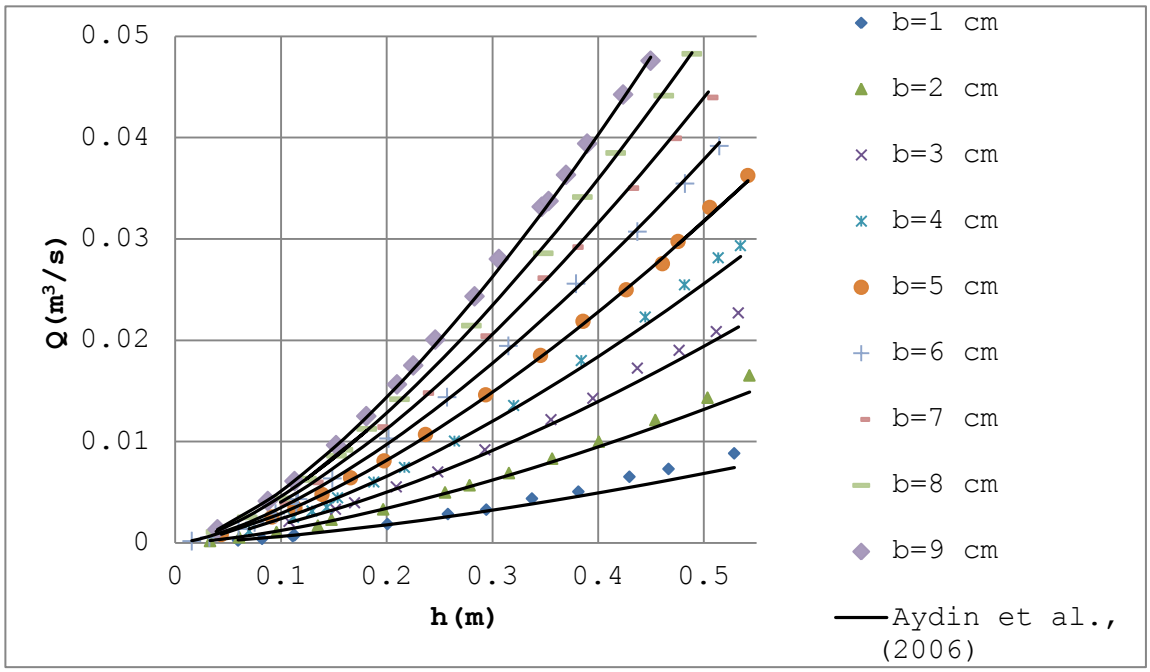

Figure 5.9 Comparison of slit weir data with Aydin et al. (2006) study

Calculation of discharge by Aydin et al. (2006) proposal is described in Section 3.5, Eq. (3.9) is used to draw the curves in Figure 5.9.

Based on their findings, a slit weir can be fitted into a channel with $B \geq 4b$ and $P \geq 0.04$ m where the discharge coefficient is only a function of Reynolds number.

Although Aydin et al. (2006) found the mentioned expression under different circumstances than the present study's, but the general overlapping occurs between the measured and calculated data with average 4.3 error percentage (The absolute value).

The error distribution is shown in Figure 5.10 with respect to experimental discharges. Eq. (5.4) is used to calculate the error. Small discharges naturally have larger errors and therefore have dominant effect on the overall error percentage. About 75 percent (92 out of 123 points) of the entire data points are confined within ±5% of error distribution range.

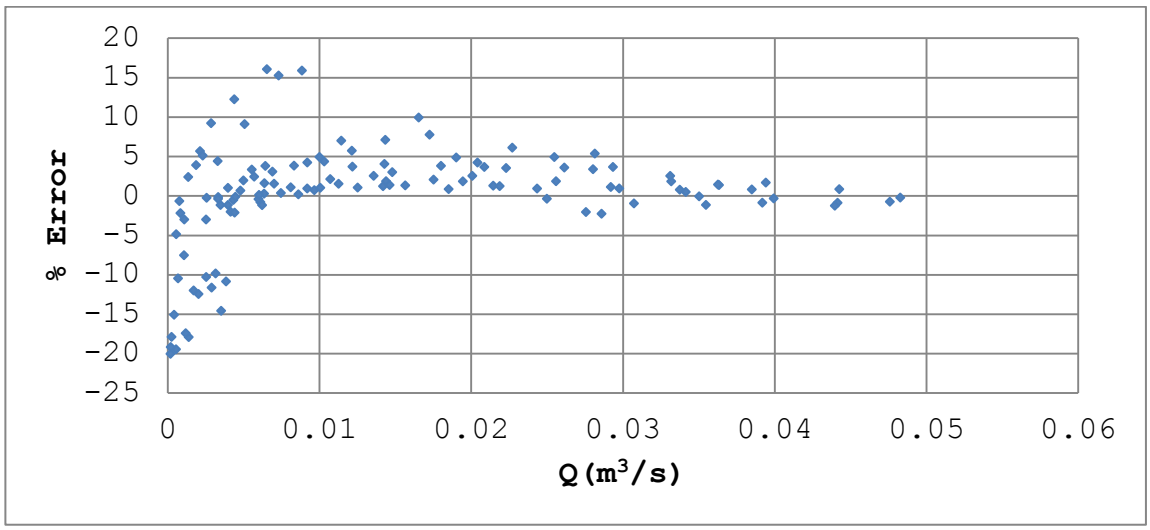

Figure 5.10 Percent error with respect to experimental discharge and Eq. (3.9)

5.2.3. Contracted Weir Case Comparison with Kindsvater and Carter, 1957

Experimental discharge coefficients are compared with Kindsvater and Carter (1957) study in Figure 5.11 for contracted weirs.

Points are representing the data and curves are drawn by Eq. (3.4) suggested by Kindsvater and Carter (1957). Details of their study are explained in Section 3.3. The consistency between the points and the curves is more acute for larger weir openings and smaller discharges, but the general agreement between the discharge values is valid throughout the whole opening gaps.

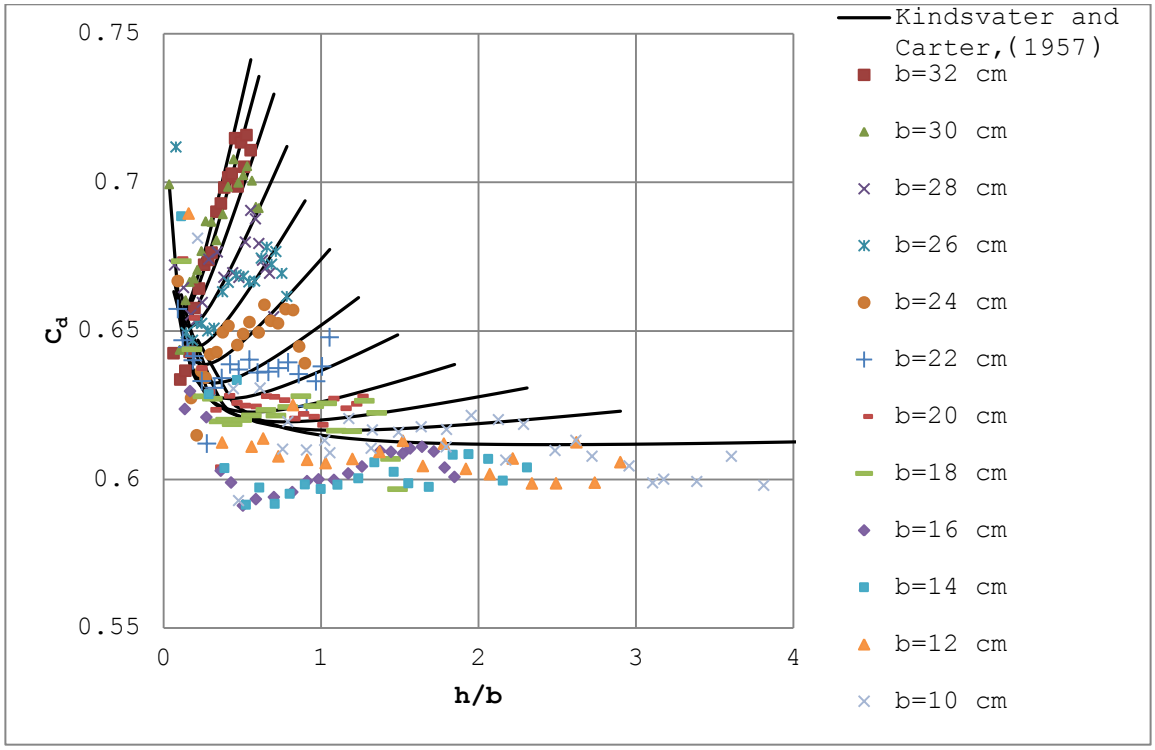

Figure 5.11 C_d variation with h/b ratio for contracted weirs

The percent error between the experimental data and the calculated discharges are demonstrated in Figure 5.12. The absolute value of overall error percentage for the whole data set is 2.57 percent. Out of 254 points, 227 points have errors less than ±5 percent. In other words, almost 90 percent of the experimental data falls within ±5% error range when compared with Kindsvater and Carter, 1957 study.

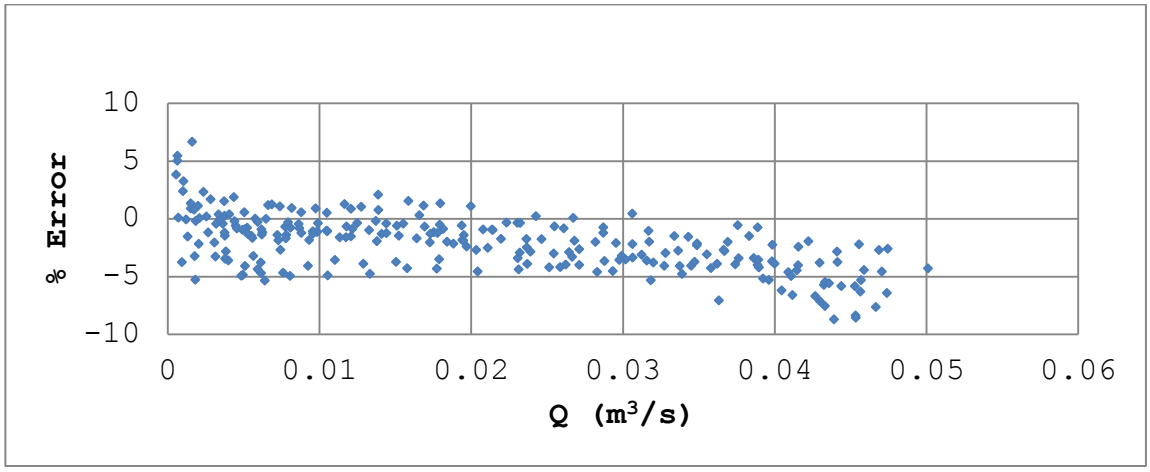

Figure 5.12 Percent error with respect to experimental discharge and Eq. (3.4)

The reason for choosing Kindsvater and Carter (1957) formula in order to make comparisons for the contracted and slit weirs is that their study is quite extensive, trustable and has been referenced in many books making it a propoer selection among other studies.

Choosing Aydin et al. (2006) study for the slit weirs comparisons is due to the fact that this study is specifically made on slit weirs and is consistent with present research.

5.3. Present Study

As, stated earlier, in discharge measurement, Eq. (2.7) is commonly used and the only unknown to be found in that equation is discharge coefficient (C_d). Whatever effort has so far been made, has mostly been to formulate the C_d in terms of other variables based on the experimental data since C_d resembles to be a convenient parameter to express the data in the frame of an equation. However, C_d has a complex behavior which makes it very difficult to illustrate it as a function of other variables (Figures 5.4, 5.5 and 5.6).

In Figure 5.13, by using Eq. (2.7), discharge coefficients for the measured data are plotted against the Reynolds number. Reynolds number for the contracted weirs is calculated by Eq. (5.2).

It can be seen that C_d changes abruptly with even small changes in R (Plotting C_d against the h/P ratio has the same feature). At the same time, different equations offered for C_d by many researchers are at odds with each other (Figure 5.14), mainly because their findings are only applicable to a limited range of data and the suggested expressions are generalized to be used for extended ranges. This claim is shown in an example in Figure 5.14, where C_d values for b/B=0.625 case are calculated through French (1986) and Bagheri and Heidarpour's (2010) suggested relations and are placed next to experimental C_d values. Looking at the figure, it is clear that none of the lines are similar to the actual trend of discharge coefficients.

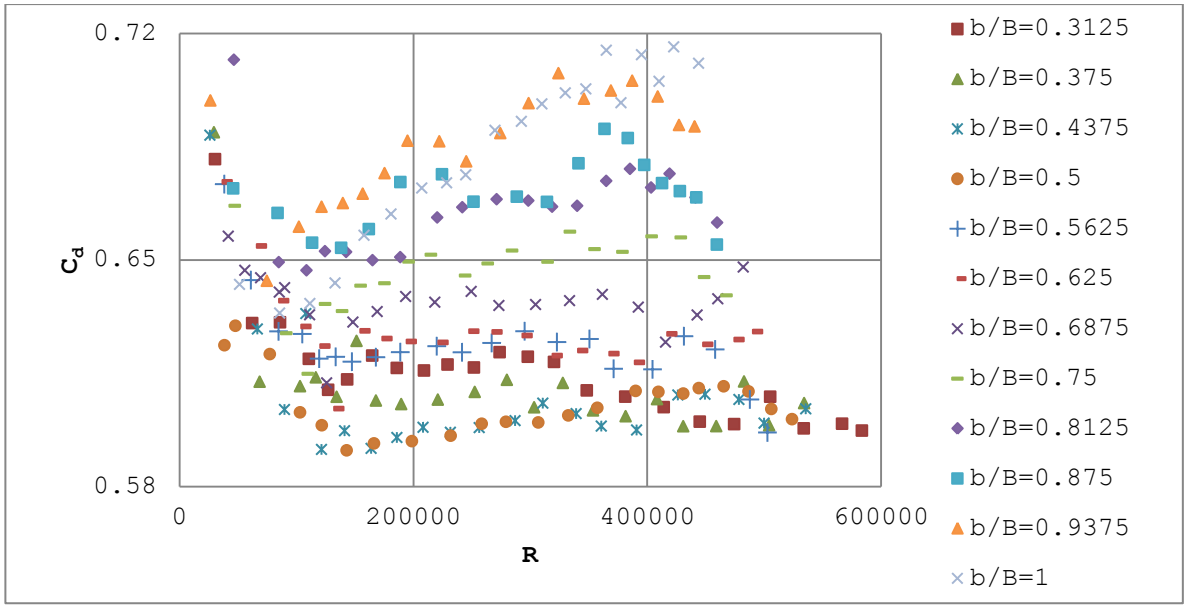

Figure 5.13 Relationship between C_d and R for contracted weir case

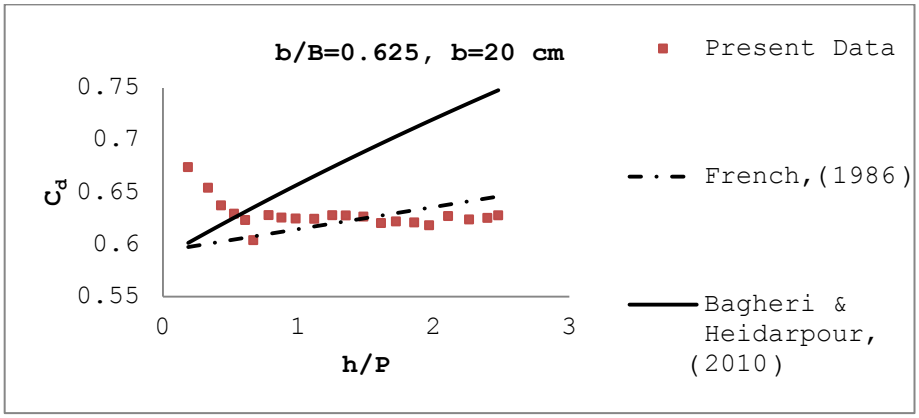

Figure 5.14 Comparison of data with previously suggested equations for C_d versus h/P ratio for b/B=0.625

Plotting weir velocity (V_w) against the weir head (h) illustrates a universal behavior which can be used in a way that can express a relationship for discharge formula (Figure 5.3). In addition, according to the same plots, it can be realized that the curves have a unique appearance from best fit point of view and by contrast, no random scatter manner is observed when compared to Figure 5.13.

Regarding the special specifications of weir velocity, formulating the discharge in terms of weir velocity seems to be easier than doing so for the discharge coefficient. Thus, in a contracted or fully contracted weir, discharge can be calculated by the Eq. (5.5):

$$\mathbf{Q = bhV_w} \qquad \mathbf{(5.5)}$$

For this purpose, a widespread search was conducted to examine and find the most simple and the best fit function for the entire data set. Among many candidate functions, power function ,Eq. (5.6) was selected for it had a higher correlation factor as well as having the simplest form of a prospective function.

$$\mathbf{V_w = ch^e} \qquad \mathbf{(5.6)}$$

where c and e are the best fit coefficients. By conducting regression analysis, it was discovered that c and e could be functions of (b/B). Applying multivariate optimization

technique with utilizing all the data sets in the problem yield to the following results:

$$c = c_1(b/B)^2 + c_2(b/B) + c_3 \quad (5.7)$$

$$e = e_1(b/B)^2 + e_2(b/B) + e_3 \quad (5.8)$$

For some reasons which will be discussed, extra constraints were imposed on the findings to better improve the functions. For example, coefficient e had a very small range in value, therefore, all of the e values (0.5759, 0.533, 0.509, 0.5146, 0.513, 0.49985, 0.491531, 0.48125, 0.5037, 0.4935, 0.5037, 0.4935, 0.4837, 0.4725 and 0.49) were averaged and a constant of 0.504 was obtained. To straighten the function, e was considered equal to constant value of 0.5. Based on theoretical considerations, velocity is proportional to square root of the available head, to make c non-dimensional, weir velocity was re-structured as Eq. (5.9):

$$V_w = c\sqrt{2gh} \quad (5.9)$$

Solving the optimization problem according to the new weir velocity equation for every weir opening (b) with the additional mentioned modifications, it was discovered that there always exists a turning point at around $0.2 < b/B < 0.5$ (range where transition from slit to contracted occurs),

requiring the c function to be split into two zones (Figure 5.15).

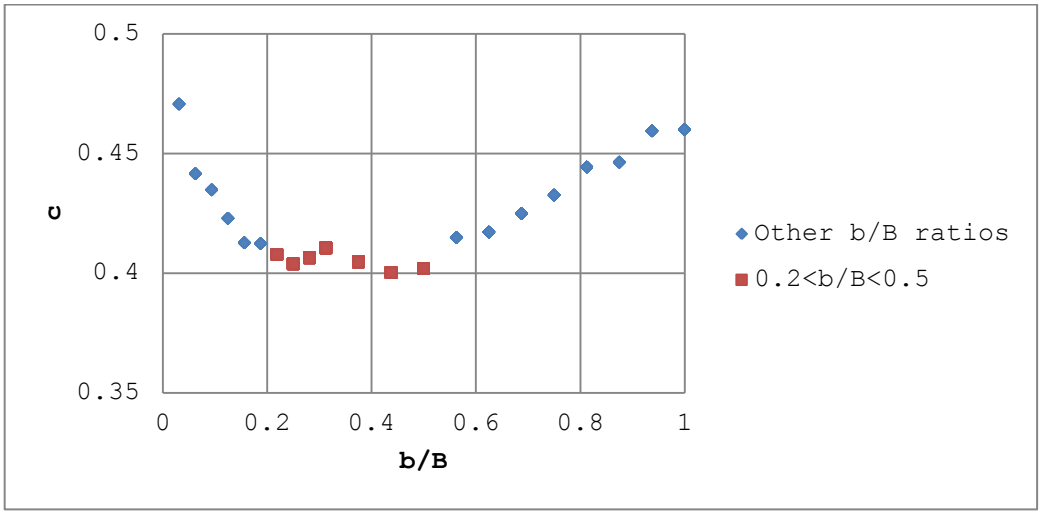

Figure 5.15 Individual c values' relation with b/B ratios for all weir openings

As it is seen from Figure 5.15, the range of 0.2< b/B <0.5 is highly sensitive to experimental errors and this will make difficulty in spotting the exact b/B ratio to separate the slit from contracted weirs, it there exists one.

However, there may lay a clue in the past studies, helping to pinpoint the range for the transition zone. The previous study on weirs by Sisman (2009) was carried out under the same experimental conditions as the present study. In order to decide on the valid transition zone range, Sisman's (2009) data were utilized and the same analysis was applied to the data. Results of the analysis for individual c values are shown in Figure 5.16. In the figure, it is seen

that almost exactly identical turning point is taking place in the 0.2< b/B <0.4 range. Since in the previous study smaller heads and thus smaller discharges were recorded, it seems that the precision of the past study was higher. Therefore, it is now possible to judge that the transition zone may be 0.2< b/B <0.4 which will be used to find the boundary b/B ratio.

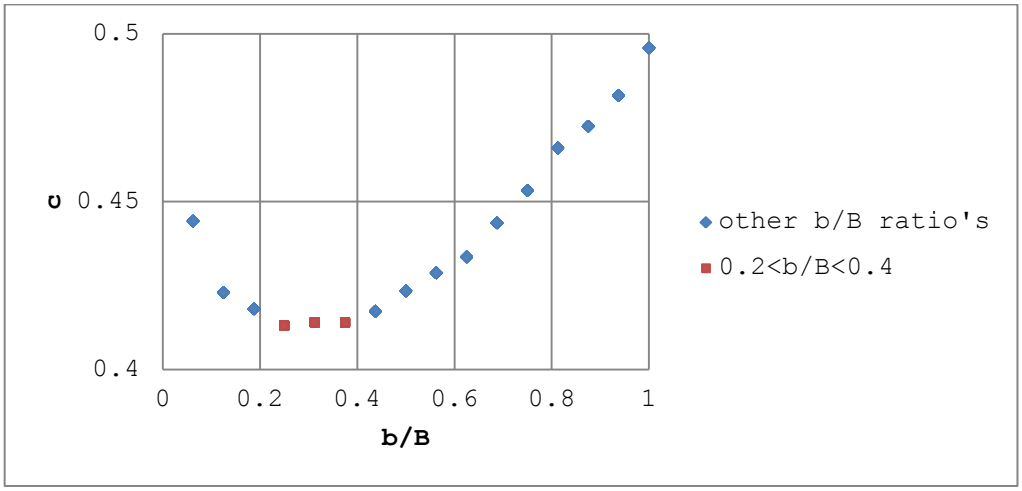

Figure 5.16 Individual c values' relation with b/B ratios for all weir openings for Sisman's (2009) data

Assuming the transition zone as 0.2< b/B <0.4 , errors in that range were minimized by considering the original function (Eq. (5.7)) to manifest the c relation with b/B for the present data:

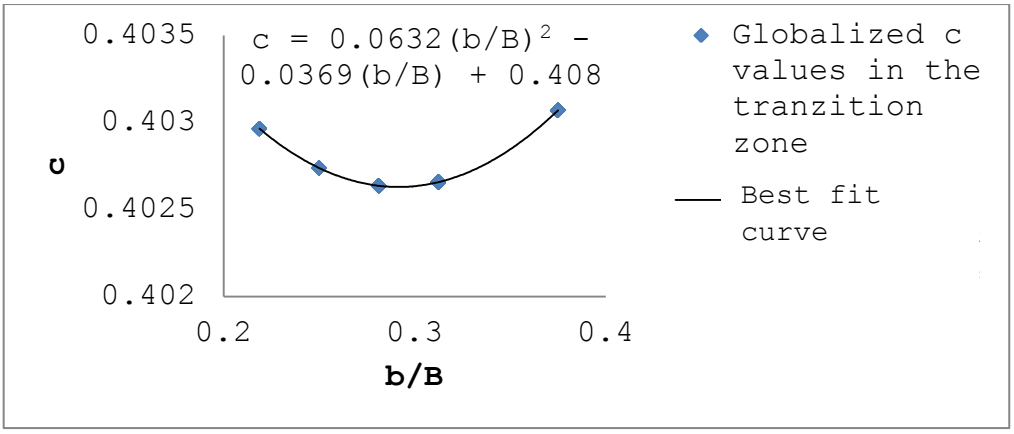

Figure 5.17 c versus b/B in transition zone

As shown in Figure 5.17, by equating the first derivative of the c function equal to zero, b/B=0.2915 ratio seems to be separating the slit and contracted weirs. For Sisman's (2009) data, same procedure lead to b/B=0.32 as the boundary of the slit and contracted weirs.

As stated before, since determining the dividing b/B ratio in the transition zone is not simple due to experimental errors, though finding it is of great importance in formulating the weir equation. The one found (b/B=0.2915) in the transition zone is neither round nor precise, thus it is best to choose the closest round ratio which is b/B=0.3. This ratio will be used afterwards to progress the rest of analysis accordingly.

Also, according to Aydin et al. (2002 and 2006), for the range b/B ≤ 0.25 flow is independent of B and weir is called slit. In the slit weirs, the average velocity of the approach channel is so small that the channel can be considered as a reservoir, minimizing the effect coming from the channel width (B) on the discharge of the weir. In the present study, somewhat a close boundary (b/B=0.3) is observed to be separating the slit and contracted weirs.

5.3.1. Formulating Weir Velocity for Slit and Contracted Weirs

Now that boundary of slit and contracted weirs is specified, using two functions for each territory would furthermore optimize the utility of the functions.

Eq. (5.9) can be written separately for contracted and slit cases:

$$V_c = c_c \sqrt{2gh} \qquad (5.10)$$

$$V_s = c_s \sqrt{2gh} \qquad (5.11)$$

Where V_c is the weir velocity for contracted weir and V_s is slit weir velocity.

The coefficients c_c and c_s are the weir velocity coefficients for contracted and slit weirs, respectively.

Re-solving the optimization problem with the new configurations, best fit coefficients are found as below:

For contracted weirs ($b/B \geq 0.3$):

$$c_c = 0.153\left(\frac{b}{B}\right)^2 - 0.0922\left(\frac{b}{B}\right) + 0.4136 \qquad (5.12)$$

and for slit weirs (b/B ≤ 0.3):

$$c_s = 0.7955\left(\frac{b}{B}\right)^2 - 0.4773\left(\frac{b}{B}\right) + 0.4712 \qquad (5.13)$$

Both of the functions can be used in the joining intersection (b/B=0.3) as shown in Figure 5.18.

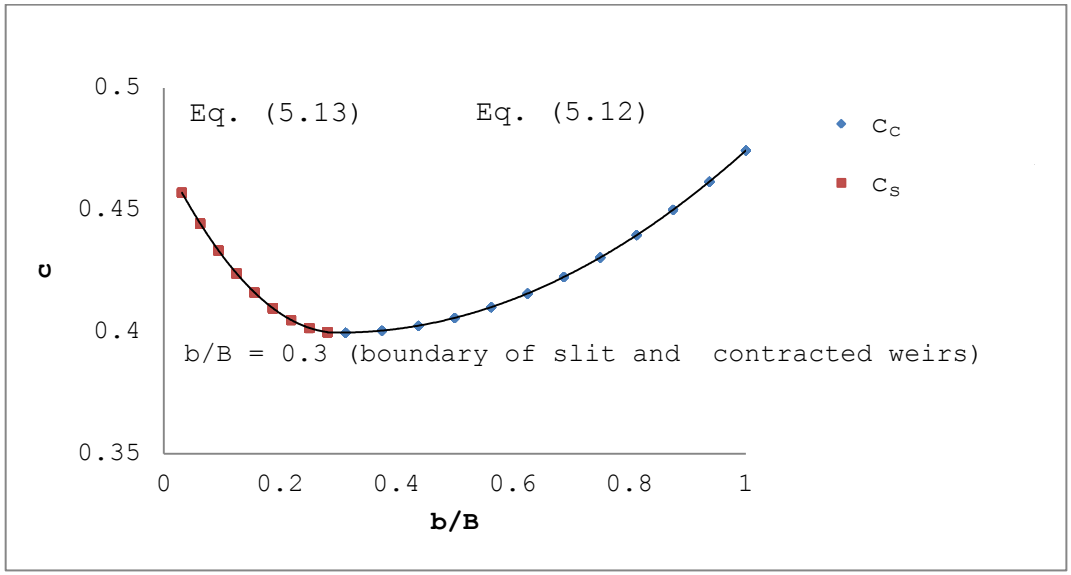

Figure 5.18 c_c and c_s versus b/B

Figures 5.19 and 5.20 are comparing the measured discharges with discharges calculated by Eq. (5.5), using contracted (Eq. (5.12)) and slit (Eq. (5.13)) coefficients suggested in the present section.

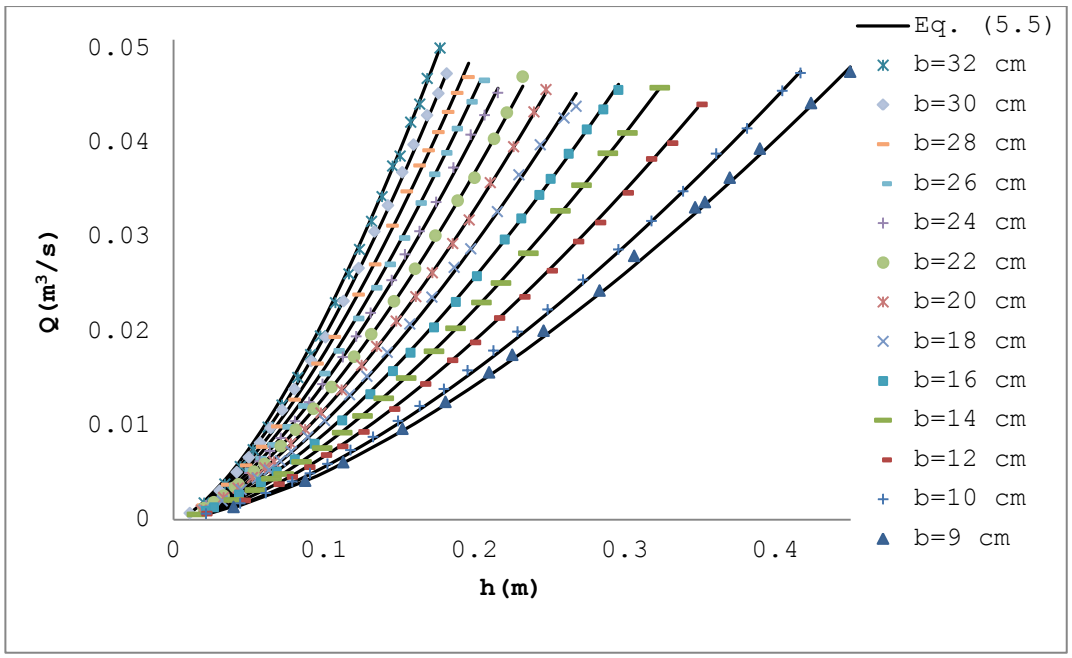

Figure 5.19 Measured discharges compared to calculated discharges for contracted weirs

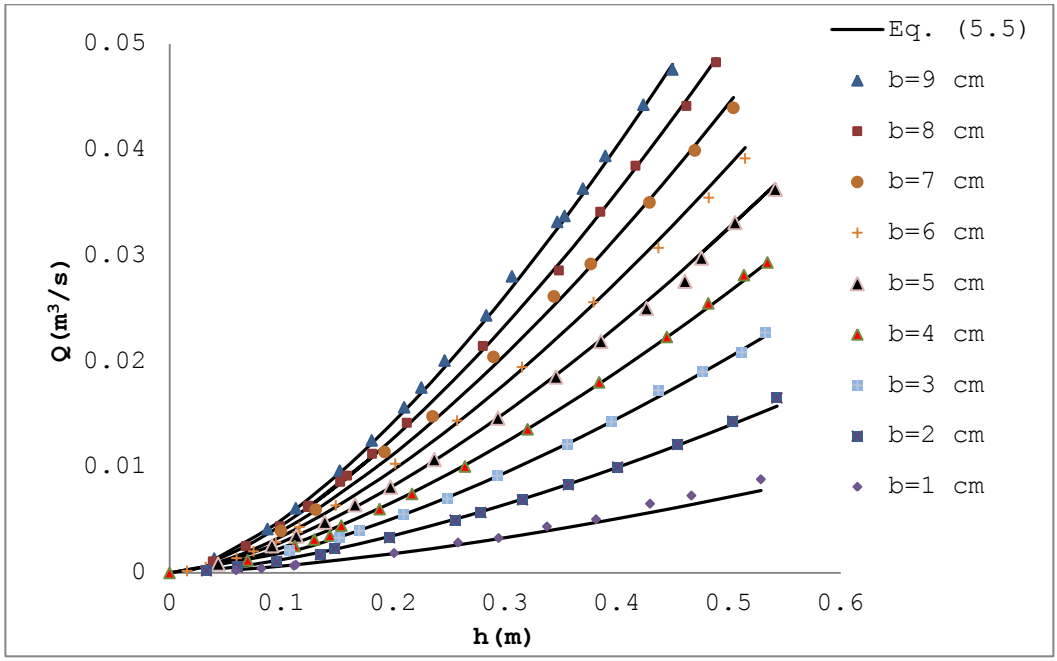

Figure 5.20 Measured discharges compared to calculated discharges for slit weirs

As it can be seen from the Figures 5.19 and 5.20, using suggested weir velocity function in discharge relation can almost precisely represent the data points.

The relative error percentage between the collected data and the calculated values, given through Eq. (5.4) are plotted against measured discharges in Figure 5.21 for the contracted weir range. It is observed that the relative error percentage for majority of the data points is around ±3%, in other words, 83 % of the entire data points have a relative error within ±3% range (There were 270 measured data points where 224 points are confined within the ±3% error range and 13 points have errors out of ±7 % range).

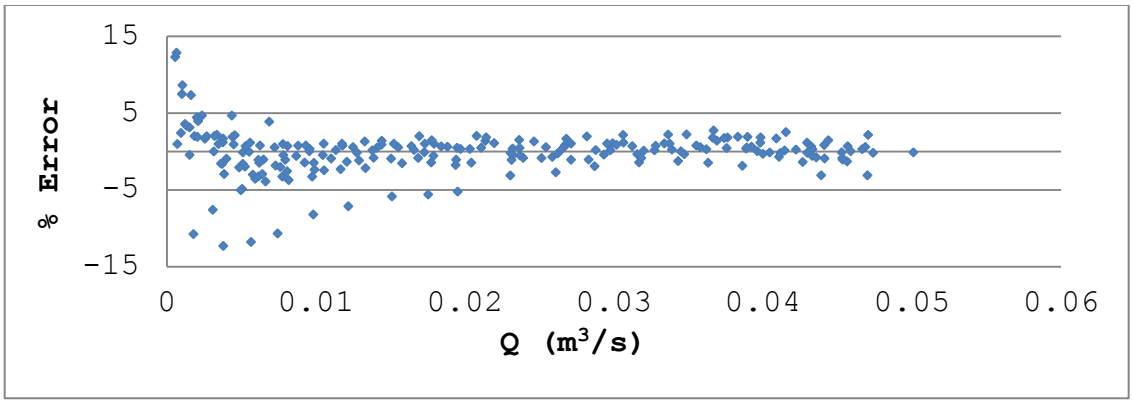

Figure 5.21 Relative error percentage between measured and calculated discharges for contracted weirs

Also in Figure 5.22, the relative error percentage between the collected data and the calculated values through Eq. (5.4) are plotted against the measured discharges. Average relative error calculated for the slit weir case for the

absolute value of difference between the measured and calculated data is around 3.99% for the whole data set. It is worth mentioning that in the slit weirs, small discharges have naturally large error percentages and therefore have dominant effect on the average error percentage and error distribution. There were 127 points collected in the slit weirs and 99 points are confined within ±5% error range, in other words 78% of the whole data points.

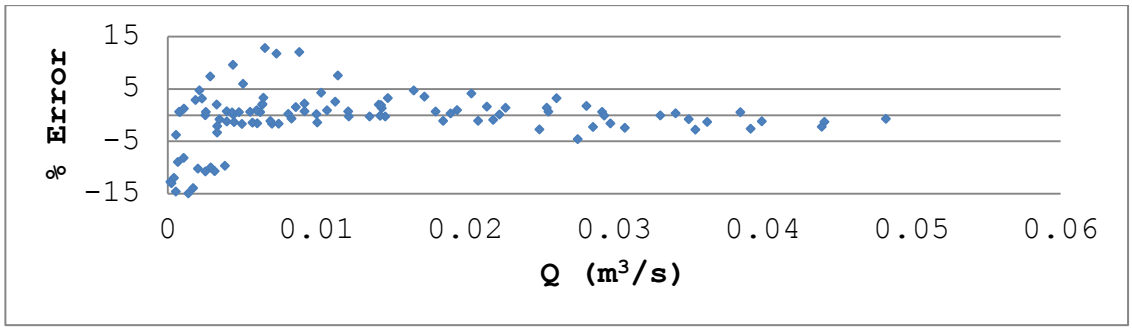

Figure 5.22 Relative error percentage between measured and calculated discharges for slit weirs

One of the experimental error sources could be linked with the exact weir opening gap adjustment and its subsequent hesitations in using that value in the analysis. That is, in some of the cases, contradictable results were received and consequently several measurements were repeated twice. It was discovered, only after careful examinations, that the weir opening space might be exposed to very little changes during the measurements in small weir openings for some reasons. In one of the cases where b=1 cm, for

example, three exact measurements were conducted using a Vernier caliper, starting from the top of the weir plate to the bottom. The b values recorded before the start of experiments were exactly 1 cm, whereas the same distance had turned to around 1.05 cm at the end of the measurements.

Looking at the problem optimistically, it is expected that such sort of errors be eliminated by the act of global optimization of the best fit function using complete data set. When weir velocity functions undergo the multivariate optimization process, illogical shifts in the trend are forced to diminish. In previously described problem with b=1 cm, by seeing the Figure 5.20, the difference between measured and calculated discharges is visible to the naked eye. The curve representing the discharges (b=1 cm) is giving a little smaller values when compared to the experimental data and that is probably because experimental discharges are corresponding to b=1.05 cm and not b=1 cm. As the weir opening gap increases, this problem is less influential though.

Regarding the composition of error shown in the figures, there may be different sources contributing. Human errors are already driven to the margin when it comes to judging between the human and flow dependent errors. Yet, human sources of error exist and they do affect the analysis in a negative way, but still they are far less influential. These kinds of errors are the ones that human can have little control over them. One of the sources can be related with the head readings. The gauge reader in the lab installation is manufactured for precise measurement with 0.1 mm of accuracy, therefore, head reading error is

limited as less than 0.1 mm. In one extreme case (smallest measured discharge, Q=0.205 l/s), for example, if 0.1 mm mistake is made in the head reading it can contribute to at most 0.45 percent error in discharge value. Another source of error is linked with precise adjustment of b (opening length of the weir crest). Due to some factors such as little deformation of the channel side walls after filling it or temperature variations, vertical weir plates may be exposed to several undesired tensions which might cause changes in the flow area of the weir section. For example, 0.1 mm change in weir length (b) can cause almost 0.5 percent error in discharge in the worst case. However, it should be emphasized that given error percentages are maximum possible values, in larger discharges and larger heads, this kind of error is almost completely ignorable.

Even if all measurement errors are eliminated, still it is difficult to claim perfect readings of head and discharge since time wise variations flow quantities, due to essentially unsteady nature of turbulent flows. There are complex turbulent flow patterns in various sections upstream of the weir plate which may sustain fluctuations of flow quantities at the measuring sections.

The error shown in Figures 5.21 and 5.22 represents some combination of all kind of errors mentioned above.

5.4. Applicability of Dressler Theory to Weir Flow

Dressler (1978) has derived governing equations of shallow, two-dimensional flow over curved faces.

Eq. (5.14) is outlined by Dressler (1978) and Sivakumaran et al. (1981, 1983) for the flow over a circular face, or circular weir in other words:

$$q = U_1 R' \ln\left(1+\frac{Y_2}{R'}\right) \qquad (5.14)$$

in which, q is the unit discharge per crest length, R' is the radius of the circular weir, U_1 is the maximum velocity on the top of the weir section and Y_2 is the water depth on the top of the weir.

U_1 can be approximated by Eq. (5.15) as:

$$u = \frac{U_1}{\left(1+\frac{y}{R'}\right)} \qquad (5.15)$$

In which, u is horizontal velocity component and y is the water depth starting from bed. Also, U_1 can be assumed as the maximum velocity at the crest which could be considered as Torricelli velocity.

The basis of Dressler theory was verified by Ramamurthy (1993) by obtaining a discharge coefficient function by

equating the general discharge equation (Eq. (2.7)) and Eq. (5.14) for circular weirs.

The same justification could have been proven to exist for the rectangular weirs. If any kind of relation had existed, rectangular weir equation might have been improved moreover. However, at the end of the experiments, such a relationship was not observed in the present study, either due to experimental shortcomings or false basis of the assumptions. But mostly, it was because of experimental infeasibilities which will be described in the next paragraphs.

When flow passes over the sharp-crested rectangular weir, somewhat a circular nappe takes shape downstream of the weir crest. This curvilinear flow might be analyzed with the help of Dressler equation by making some assumptions.

For this purpose, several measurements on nappe profiles and water head on the crest were performed. Radius of the lower nappe formed under the jet was measured for different weir widths and water heads. It may be assumed that in Eq. (5.14), Y_2 is the water depth right on the crest. Then the mentioned term can be replaced by a simple function which is dependant on weir opening and upstream water head- the parameters that are much easier to measure- as shown in Figure 5.23.

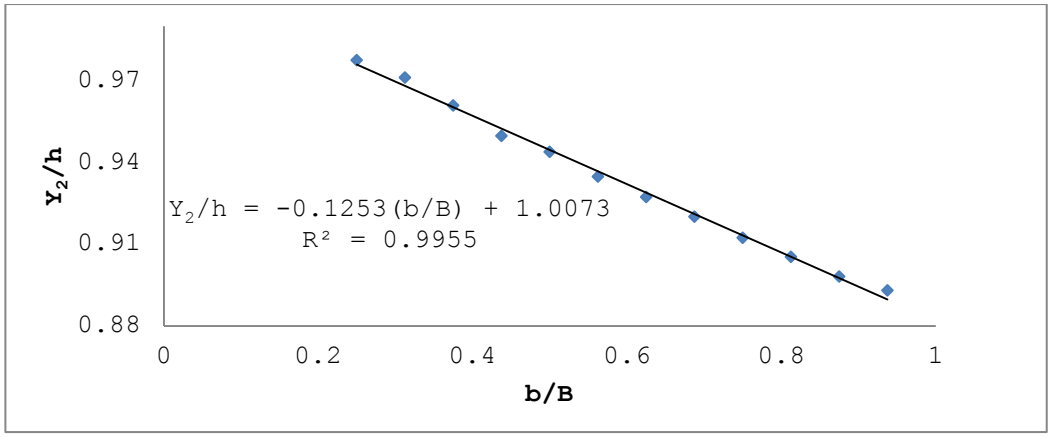

Figure 5.23 Variation of Y_2/h with b/B ratio

By contrast, it was revealed that nappe radius did not have any logical relation with other parameters as shown in Figure 5.24 (At least from best-fit point of view). Therefore, no appropriate function for nappe radius was found to place it in the Eq. (5.14) and see if the discharge is actually given by the Dressler equation for rectangular weirs.

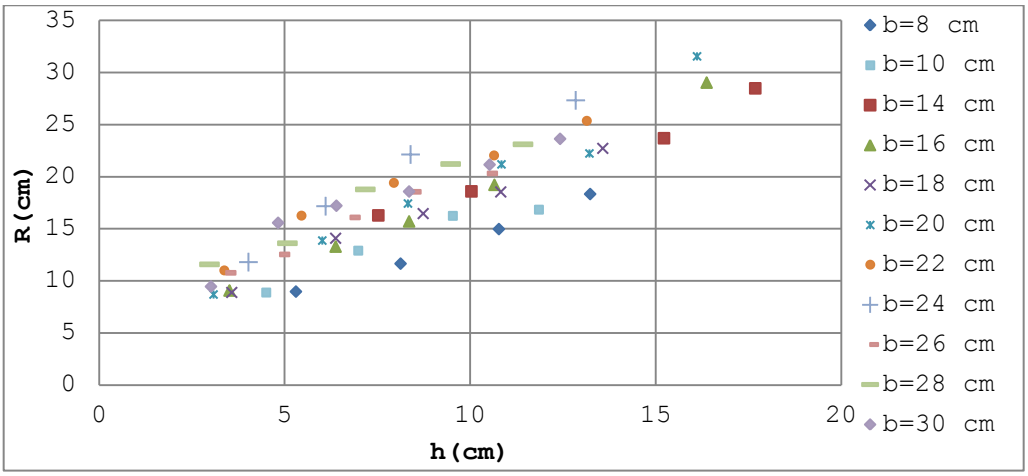

Figure 5.24 Variation of nappe radius with water head for different weir openings

Even though, water depth at the crest is smoothly linked with b and h, but in larger heads and smaller weir openings measuring the depth was very difficult. Looking at Figure 5.25, it is easy to imagine that in the center of the weir opening water surface is very oscillatory.

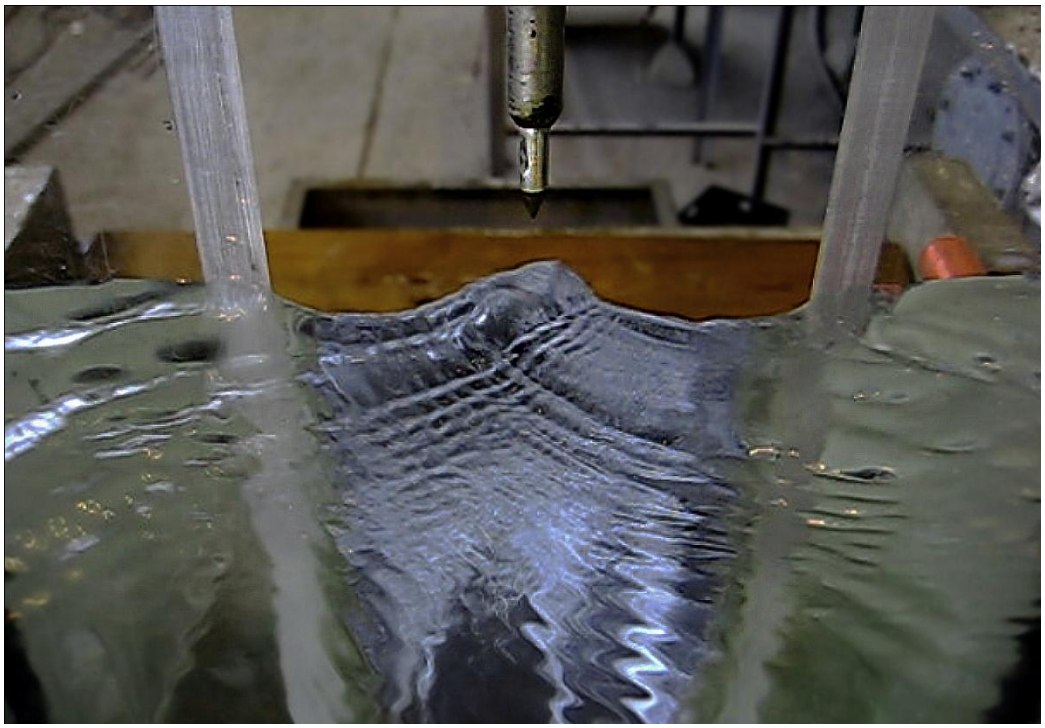

Figure 5.25 Oscillation of water surface at the weir exit

For nappe radius measurement, a simple camera was used. The camera's focal point was pointed perpendicular to the nappe. For a variety of weir openings and water heads, pictures were taken and then they were processed in AutoCAD software to find the radiuses. Figure 5.26 shows one

typical picture of nappe along with its radius-finding step:

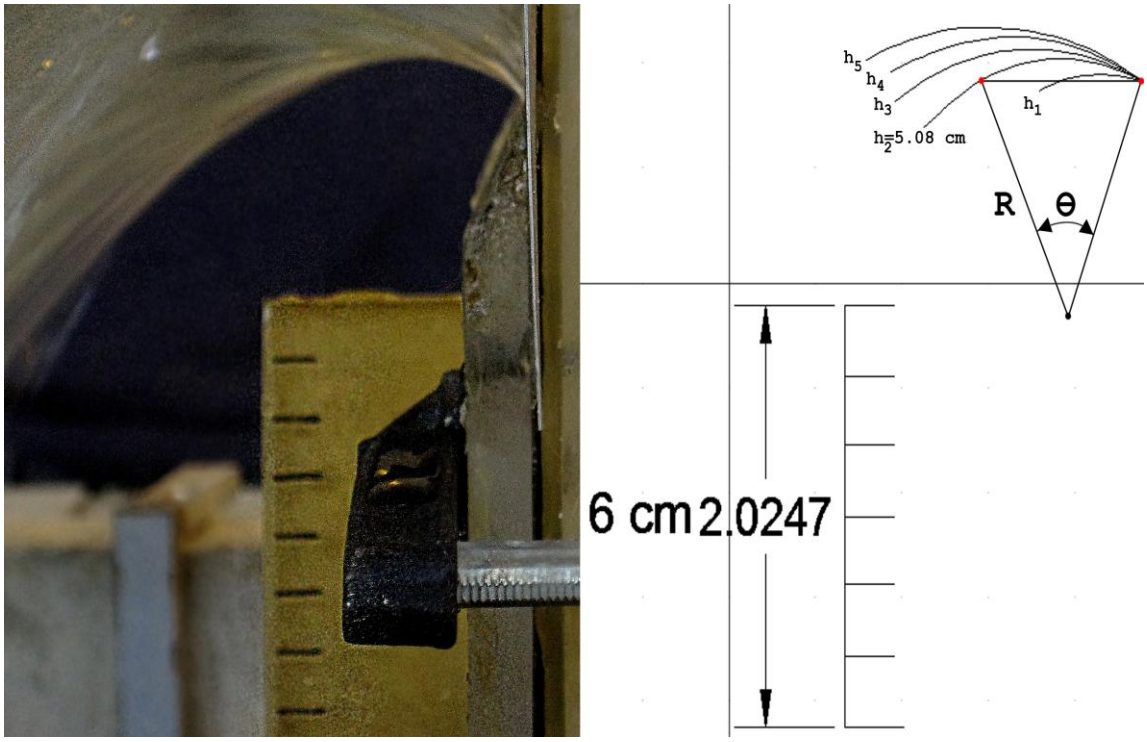

Figure 5.26 A typical picture of nappe

CHAPTER 6

CONCLUSIONS

This study is an experimental investigation on sharp-crested rectangular weirs. This research was developed based on an empirical approach to seek the contributions of a newly introduced 'weir velocity' concept to improve and simplify the weir discharge equation.

Conclusions of the present study are listed below:

1- For full width channel, several tests were performed on different weir heights to see the effect of plate height on the discharge capacity when plotted against the available head. Weir plate height, P of 10 cm was chosen as the one which suppresses the boundary layer growth for the discharge (or head over weir) range studied.

2- As already discussed, sharp crested rectangular weirs are fallen into two major categories, slit and contracted weirs. In the present study, the separating b/B ratio was approximately found to be equal to 0.3. Variation of the weir velocity coefficient with b/B ratio proves that there is a shift in the behavior of the weir at around b/B=0.3, separating the contracted weirs from slit weirs.

3- In the discharge expression where discharge coefficient (C_d) is dropped, weir velocity plays the key role (Eq. (5.5)). After performing widespread analysis on the experimental data along with regression analysis, discharge relation and its best fit non-dimensional coefficients were found as already mentioned in Chapter 5 as in Equations. (5.10), (5.11), (5.12) and (5.13).

   By looking at the extracted weir velocity (Eq. (5.9)), it is noticed that as potentially expected, velocity term is identical to Torricelli velocity with only a non-dimensional correcting constant multiplied to it, where that constant is itself a function of b/B ratio.

4- In contracted weirs, where flow is driven mainly by gravity and inertia forces, b/B ratio could be one of the important parameters in representing the gradual transition of streamlines from parallel to curved state suggesting the pattern behind discharge reduction trend. But in slit weirs, where Reynolds number and surface tension effects are impossible to deny, b/B ratio might not be faithfully displaying the corresponsive relation between the discharge and weir opening. With all these considerations, larger errors in the small discharges may not only be due to the

tininess of the discharges, but also might be due to the probable underestimations of those secondary forces mentioned. This truth can leave room for future revisions and improving of the slit weirs expression. Nevertheless, results given by the present function, proposed for slit weirs, is not outlying by a great magnitude when compared to the results of some of the earlier leading studies. It is worth mentioning that the given functions in the present study are by far simple and compact in outlook when compared to the earlier studies.

REFERENCES

Aydin, I., Ger, A. M. and Hincal, O. (2002). "Measurment of Small Discharges in Open Channels by Slit Weir." Journal of Hydraulic Engineering. ASCE; Vol. 128, No. 2,234-237.

Aydin, I., Altan-Sakarya, A.B. and Ger, A.M. (2006). "Performance of slit weir.". Journal of Hydraulic Engineering. ASCE;Vol. 132, No. 9, 987-989.

Aydin, I., Altan-Sakarya, A.B. and Sisman, C. (2011). "Discharge formula for rectangular charp-crested weirs." Journal of Flow measurement and instrumentation. Vol. 22, No. 22, 144-151.

Bagheri, S. and Heidarpour, M. (2010). "Flow over rectangular sharp-crested weirs." Journal of irrigation Science. Vol. 28, 173-179.

Bos, M. G. (1989). "Discharge Measurment Structures." International Institute for Land Reclamation and Improvement, Third Edition, Wageningen, The Netherlands.

Chow, V. T. (1959). “Open Channel Hydraulics.” McGraw-Hill Book Company Inc., Newyork.

Dressler, R. F. (1978). “New Nonlinear Shallow Flow Equations with Curvature” Journal of Hydraulic Research. IAHR, Vol. 96, No. 3, 205-222.

Franzini, J. B. and Finnemore, E. J. (1997). “Fluid Mechanics with Engineering Applications.” McGraw-Hill Company Inc.

French, R.H. (1986). “Open channel hydraulics.” McGraw-Hill, New York.

Henderson, F.M. (1966). “Open channel flow.” Prentice-Hall Inc.

Kandaswamy, P. K. and Rouse, H. (1957) “Characteristics of Flow Over Terminal Weirs and Sills.” Journal of of Hydraulics Division, Vol. 83, No. 4, August, 1-13.

Kinsdvater, C. E. and Cater, R. W. (1957). “Discharge Characteristics of Rectangular Thin-Plate Weirs.” Journal of Hydraulics Division, Vol. 83, No. 6, December, 1-36.

Munson, B. R., Young, D. F. & Okiishi, T. H. (2002). “Fundamentals of Fluid Mechanics.” John Wiley & Sons Inc., New York, USA.

Ramamurthy, A. S., Tim, U. S. and Rao, M. V. J. (1987). "Flow over Sharp Crested Plate Weirs." Journal of Irrigation and Drainage Engineering, Vol. 113, No. 2, 163-172.

Ramamurthy, A. S. and Ngoc-Diep, V. (1993). "Application of Dressler Theory to Weir Flow." Journal of Applied Mechanics, Vol. 60, 163-166.

Ramamurthy, A. S., Qu, J., Zhai, C. and Vo, D. (2007). "Multislit Weir Characteristics." Journal of Irrigation and Drainage Engineering, Vol. 133, No. 2, 198-200.

Rehbock, T. (1929). "Discussion of precise weir measurement" by E.W. Schoder and K.B. Turner. ASCE, Vol. 93, 1143-1162.

Rouse, H. (1936). "Discharge Characteristics of the Free Overfall." Civil Engineering. ASCE, Vol. 6, No. 4, 257-260.

Sisman, C. (2009). "Experimental Investigation on Sharp-Crested Rectangular Weirs." M.Sc. Thesis, department of Civil Engineering, Middle East Technical University, Ankara, Turkey.

Sivakumaran, N. S., Hosking, R. J. and Tingsanchali, T. (1981). ”Steady Shallow Flow Over a Spillway.” Journal of Fluid Mechanics, Vol. 111, 411-420.

Sivakumaran, N. S., Tingsanchali, T. and Hosking, R. J. (1983). “Steady Shallow Flow Over Curved Beds.” Journal of Fluid Mechanics, Vol. 128, 469-487.

Sturm, T. W. (2001). “Open Channel Hydraulics”. McGraw-Hill Book Company Inc., New York.

Swamee, P. K. (1988). “Generalized Rectangular Weir Equations.” Journal of Hydraulic Engineering, Vol.114, No. 8, 945-949.